Physiology and Molecular Biology of Plants (August 2023) 29(8):1205–1224
https://doi.org/10.1007/s12298-023-01351-3

RESEARCH ARTICLE

Aridity-driven changes in structural and physiological characteristics of Buffel grass (*Cenchrus ciliaris* L.) from different ecozones of Punjab Pakistan

Amina Ameer[1] · Farooq Ahmad[1] · Naila Asghar[1] · Mansoor Hameed[1] · Khawaja Shafique Ahmad[2] · Ansar Mehmood[2] · Fahim Nawaz[3] · Muhammad Asif Shehzad[4] · Sahar Mumtaz[5] · Muhammad Kaleem[1] · Ummar Iqbal[6]

Received: 2 June 2023 / Revised: 4 August 2023 / Accepted: 21 August 2023 / Published online: 21 September 2023

Abstract

Cenchrus ciliaris L. is a perennial grass that can grow in a diverse range of habitats including challenging deserts. The purpose of the study was to investigate the impact of aridity on morpho-anatomical and physiological traits in C. *ciliaris* populations collected from arid and semi-arid areas of Punjab, Pakistan. The populations growing in extremely arid conditions displayed a range of structural and physiological adaptations. Under extremely dry conditions, root epidermal thickness (90.29 µm), cortical cell area (7677.78 μm^2), and metaxylem cell area (11,884.79 μm^2) increased while root pith cell area (2681.96 μm^2) decreased in tolerant populations. The populations under extremely aridity maximized leaf lamina (184.21 µm) and midrib thickness (316.46 µm). Additionally, highly tolerant populations were characterized by the accumulation of organic osmolytes such as glycinebetaine (132.60 µmol g^{-1} FW) was increased in QN poulations, proline (118.01 µmol g^{-1} F.W) was maximum in DF populations, and total amino acids (69.90 mg g^{-1} FW) under extreme water deficit conditions. In arid conditions, abaxial stomatal density (2630.21 µm) and stomatal area (8 per mm^2) were also reduced in DF populations to check water loss through transpiration. These findings suggest that various parameters are crucial for the survival of *C. ciliaris* in arid environments. The main strategies used by *C. ciliaris* was intensive sclerification, effective retention of ions, and osmotic adjustment through proline and glycinebetaine under arid conditions.

Keywords Anatomical modifications · Sclerification · Ion accumulations · Osmotic adjustment · Aridity

Introduction

Aridity adversely affects plant survival and yields on a global scale (Hamid et al. 2020). Arid and semi-arid environments are characterized by high temperatures and low precipitation (Waseem et al. 2021). In Pakistan, more than 80% of regions are arid or semi-arid, where crop production is limited by extreme weather and unpredictable rainfall (Berdugo et al. 2020). As a result of changing environmental factors, like temperature fluctuations and alterations in rainfall patterns, crop yields in arid and semi-arid regions are significantly reduced (Lian et al. 2021). In addition, desert plants face conditions such as drought, high temperature, and salt stress. These plants have developed unique morphological and anatomical characteristics that allow them to cope with these stresses (Mumtaz et al. 2021a; b).

Plants have developed several strategies to cope with water deficiency. Anatomical changes such as increased leaf

✉ Khawaja Shafique Ahmad
ahmadks@upr.edu.pk

[1] Department of Botany, University of Agriculture Faisalabad, Faisalabad 38000, Pakistan

[2] Department of Botany, University of Poonch Rawalakot, Rawalakot 12350, AJK, Pakistan

[3] Research School of Biology, The Australian National University, Canberra, Australia

[4] Institute of Plant Breeding and Biotechnology, MNS University of Agriculture, Multan 66000, Pakistan

[5] Division of Science and Technology, Department of Botany, University of Education, Lahore 54770, Pakistan

[6] Department of Botany, The Islamia University of Bahawalpur, Rahim Yar Khan Campus, Bahawalpur 64200, Pakistan

sclerification and leaf succulence are critical for the survival of several grass species under drought stress (Mumtaz et al. 2021a, b). Drought-tolerant grasses also exhibit distinctive anatomical traits such as larger bulliform cells and wider metaxylem vessels (Waseem et al. 2021). Bullifom cell development is a significant structural modification that plays a vital role in turgor maintenance under drought (Mumtaz et al. 2019). The development of parenchyma is a very important adaptation that not only provides mechanical support (Kaleem and Hameed 2021) but also minimizes evaporation. The length of the xylem vessel is also an important indication of various environmental stresses, like heat and drought (Ali et al. 2020).

Plants develop several physiological changes under water-deficit conditions that not only prevent or reduce water loss but also absorb water necessary for plant growth and survival under limited moisture conditions (Ahmad and Haddad 2011). As a result of drought stress, soluble compounds, or compatible solutes, reduce or equalize intracellular and external ions, which are composed of amino acids, glycerols, sugars, and other molecules of low molecular weight (Hussain et al. 2022). The osmotic adjustment is mostly brought by inorganic ions i.e., Na, K, Ca, and Cl (Asghar et al. 2021). The mechanism of osmotic adjustment also reduces the ionic toxicity within the cytoplasm by limiting Na influx and its sequestration inside the vacuole (Rehman et al. 2019).

The survival of plants in desert conditions depends primarily on water availability. To gain a better understanding how plants physiological and biochemical responses to drought stress, we selected *C. ciliaris* L. (drought-tolerant forage grass) widely distributed throughout arid and semi-arid regions of the world. *C. ciliaris* L. (Buffel grass) is a common perennial grass that is widespread in water-deficit environments (Hamid et al. 2020). This grass has ability to grow in severely dry conditions and has a natural tendency to propagate in regions characterized by semi-arid and arid climates, particularly in soils that are dry, sandy, or sandy loamy (Marshall et al. 2012). It is grown as a pasture grass with exceptional tolerance to drought worldwide, because of its drought olerance capacity, rapid growth, large root system, and ability to withstand overgrazing pressure (Wasim and Naz 2020). *C. ciliaris* has immense potential for the usage, management, and stabilization of water and nutrients and ecosystem services (Mansoor et al. 2019). Most of the researchers primarily investigated its suitability as a forage plant, there is a lack of information in our understanding about the ecological behaviour of this grass in natural habitats (Ahmad et al. 2020).

Understanding how *C. ciliaris* responds to water scarcity can provide valuable insights for developing more resilient crops that can withstand drought conditions. This knowledge could enhance agricultural productivity in regions prone to water deficits thereby contributing to food security. This study was conducted to test the hypothesis that different populations of *C. ciliaris* adapt differently to various ecological zones through modifications in their structural and functional setups. To comprehend the changes in key functional traits of *C. ciliaris* under water deficit conditions, two populations from semi-arid and arid zone was studied along an aridity gradient. The purpose of this study was to compare these populations for anatomical and physiological differences in terms of structural and functional response under water scarcity.

Material and methods

Study area

The study area lies between latitude 28–35° N and longitude between 70 and 76° E and the altitude ranges from 300 to 2100 m asl (Fig. 1). These arid regions of Punjab province are considered critical to the changes in plants brought by extreme aridity. Aridity is continuously shifting from the southern to northern areas of Punjab due to global climate change. In Punjab, there is a subtropical monsoon climate. The variation of the yearly average temperature is from less than 7–12°C in the cold zone to more than 25°C in the warmer lowlands. The monsoon, often known as the wet season, lasts from July through September. The sub-mountain region has 96 cm of annual rainfall on average, whereas the plains receive 46 cm. The ratio of rainfall fluctuates up to 50 mm every month roughly throughout the remaining months (Zahid and Rasul 2012; Javid et al. 2020).

Plant material

In this study, 12 different sites covering arid and semi-arid regions were selected from Punjab province, Pakistan. From each site, three populations of *C. ciliaris* were collected during March 2019–April 2020 and replicated to evaluate their morpho-anatomical and physiological adaptations. Study sites were located about 55 km from each other. Semi-arid sites include KG (Kanhati mountains), KT (Katha), SG: (Sargodha), HT (Head Trimu), and HR (Head Rasul), whereas arid sites include SA (Salmani Adda), CA (Chock Azam), GW (Gutwala), DA (Darbar Anayat Shah), HP (Hasilpur), DF (Derawer Fort), and QN (Qila Nawab Din). Topographic and climatic variability of collection sites are presented in Table 1.

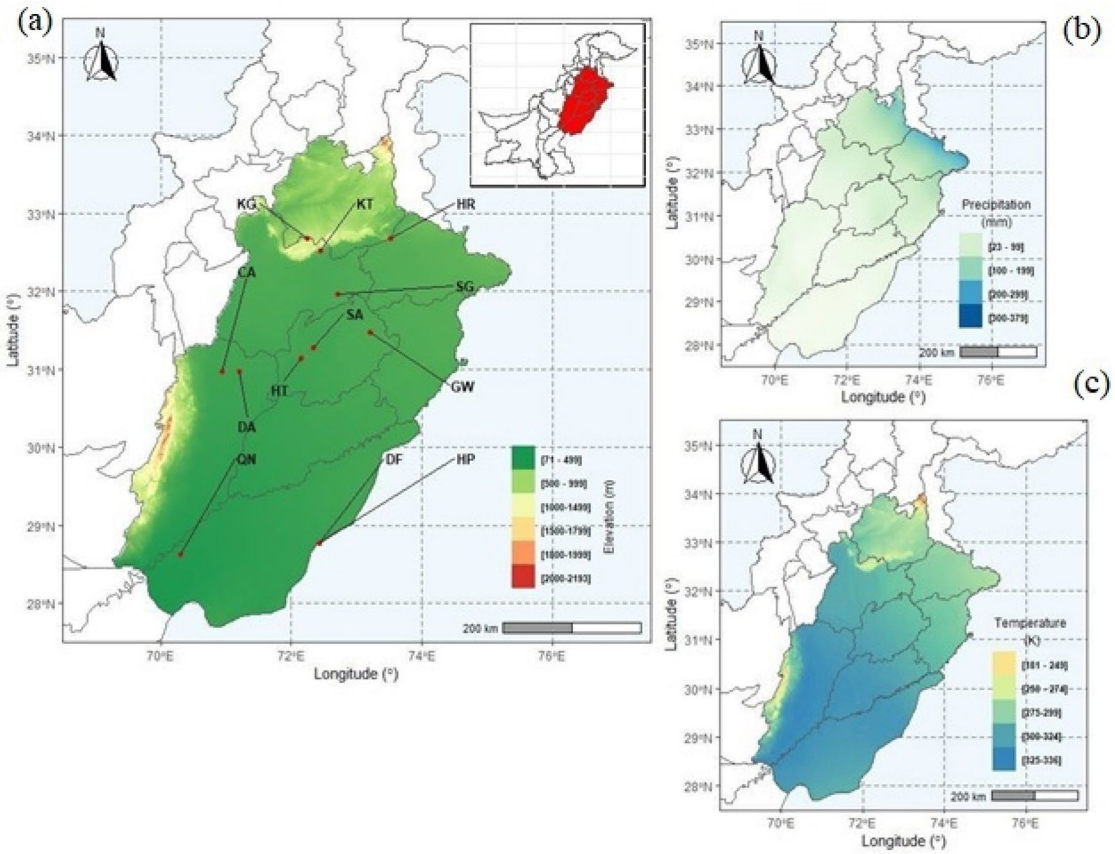

Fig. 1 Map of the study area showing **a** Locations and elevation range in the study area, **b** Variations in precipitation, and **c** Variations in average temperature. KG, Kanhati Mountains; KT, Katha; SG, Sargodha; HR, Head Rasul; GW, Gutwala; SA, Salmani Adda; HT, Head Trimu; CA, Chock Azam; DA, Darbar Anayat Shah; QN, Qila Nawabdin; DF, Derawer Fort; HP, Hasilpur

De Martonne aridity index (IDM)

De Martonne index was formulated at the beginning of the twentieth century by a French researcher Emmanuel de Martonne (Coscarelli et al. 2004). The index can be calculated on an annual basis or even more frequently. It was calculated as follows for annual values.

Table 1 Topographic and relief factors of *Cenchrus ciliaris* collection sites in the Punjab, Pakistan

Sites	Soil texture	Temperature (°C)		Annual precipitation (mm)	Annual humidity (%)	Average sun shine hours per year	Rainy days per years	Habitat ecology
		Max temp.	Min temp.					
Kanhati Mountains	Sandy loam	36	24	441	54	4082	48.5	Stony mountains
Katha	Sandy loam	38	24	404	53	4081	48.21	Foot hills
Sargodha	Sandy loam	39	24	401	50	4380	47.78	Hot and arid environment
Gut Wala	Clay loam	39	25	385	41	3963	46.71	Saline arid barren area
Head Trimu	Loamy sand	40	25	385	40.4	4383	45.22	Roadside
Head Rasul	Sandy laom	40	25	372	40	4386	45.56	Roadside
Salmani Adda	Sandy loam	41	26	286	28	4119	42.21	Tha- desert margins
Chock Azam	Loamy sand	41	26	275	26	4121	32.87	Sandy desert
Darbar Anyat Shah	Loamy sand	41	27	274	24	4122	31.36	Sandy desert
Hasilpur	Sandy loam	41	27	145	30	4125	24.32	Hot and dry environment
Derwar Fort	Loamy sand	44	28	143	27	4365	22.1	Sand dune desert
Qila Nawab din	Loamy sand	45	28	101	22.5	4371 s	20.1	Sand dune desert

$$\text{IDM} = \frac{\text{P}}{T\text{a} + 10}$$

Based on de Martonne aridity index (Table 2), the collection sites were named as Head Rasul (HR: 10.05), Kanhati mountains (KG: 11.9), Head Trimu (HT: 10.20), Katha (KT: 10.63), Sargodha (SG: 10.28), and Gutwala (GW: 10.23), fall into semi- arid zone, while Salmani Adda (SA: 7.15), Chock Azam (CA: 6.7), Darbar Anayt Shah (DA: 6.2), Hasilpur (HP: 2.9), Derawar Fort (DF: 2.8) and Qila Nawab Din (QN: 1.2) falls in arid zone (Fig. 1).

Morphological and anatomical traits

Root and shoot weights were measured with a digital balance, while lengths were recorded with a measuring scale. Fresh weight was determined immediately utilizing a weighing balance at the precision of 0.0001 g. Leaves were consequently dried to constant weight at 60 °C in an oven to determine dry weights.

For structural studies, root, stem, and leaf plant samples were taken and instantly kept in a formalin acetic alcohol (FAA) solution according to (Ruzin 1999). Permanent slides were made by free-hand sectioning. Transverse sections were dehydrated in a variety of ethanol grades and contrast between different tissue systems was developed using the biological stains safranin (1%) and fast green (5%) with 95% ethanol. The photographs of sections were taken by camera (Nikon 104, Japan) fitted with a light microscope (Leica, DM2500, Germany). Briefly, 4–5 photographs of each section were taken randomly to assess five measurements per photograph.

For stomatal traits, the center of the epidermis of the leaf surface was rubbed with a sharp blade to make a transparent imprint of leaves (Liu et al. 2019). The photographs of stomatal slides were randomly taken under a light microscope. Stomatal density (pores mm^2) was measured by considering the number of stomata on each uniform-size sample from 2 to 3 different fields of view. SD was calculated using the following equations: $SD = N/1.12 \times 10^{-2}$, where 1.12×10^{-2} represents the photograph area (mm^2).

Organic Osmolytes

For osmolyte determination, fresh samples of plants were collected at the site of collection, kept in a zipper bag, and then placed in the icebox for further analysis of glycine betaine proline total free amino acids, total soluble sugars, and soluble proteins.

Table 2 Type of climatic zones according to the de Martonne aridity index (IDM, adapted after Baltas and modelling (2007)

Climate type	IDM values
Arid	IDM < 10.0
Semi-arid	IDM < 20.0

Glycine betaine

Fresh leaf (0.25 g) was macerated in distilled 5 mL water. The extract obtained was centrifuged on an ultracentrifugation machine at 12,000 rpm for 15 min. 500 µL of a mixture (1 mL sample + 1 mL 2 NH_2SO_4) was added to each test tube and placed in ice for 90 min, followed by the addition of 200 µL potassium triiodide, 2.8 mL distilled water and 6 mL 1, 2-dichloroethane (Grieve and Grattan 1983). Finally, absorbance was recorded at 365 nm using UV-spectrophotometer (Hitatchi, 220, Japan).

Proline determination

Proline content was estimated following Bates et al. (1973). For this, frozen leaf tissues (200–220 mg) of each sample were crushed and homogenized with 3% of 4 ml aqueous sulpho-salicylic acid. The extract was centrifuged at 10,000 × *g* (Eppendorf 5804R, Germany) for 15 min. at 4 °C. After adding 2 ml of acid ninhydrin and 2 ml of glacial acetic acid in 2 ml supernatant, glass tubes were subjected to heat in a water bath at 95 °C for 1 h. The reaction tubes were placed in an ice bath for cooling. Then 4 ml of toluene was added to the reaction mixture. The reaction tubes were stirred continuously for 15–20 s. at room temperature and left undisturbed for about 30 min. Two phases were formed, the upper phase containing toluene was separated with a micropipette and its absorbance was taken and read at 520 nm using a spectrophotometer (Hitatchi, 220, Japan). A standard curve of toluene was used for the estimation of proline concentration**.**

Total soluble sugars determination

Total soluble sugars were determined using the modified method of Yemm and Willis (1954). Briefly, 200 mg of frozen leaves were crushed and homogenized with 5 ml of chilled 80% ethanol. The extract was centrifuged at 15,000 × *g* (Eppendorf 5864R, Germany) for 15 min at 4 °C. After adding 2 ml of chilled 0.2% anthrone reagent (0.2 g anthrone in 100 ml of 72% sulphuric acid) in 100 µl supernatant in glass tubes with continuous stirring for 15–20 s, the reaction tubes were heated in a water bath at 95 °C for 10 min. Absorbance was checked and recorded at 620 nm using a spectrophotometer (Hitachi, 220, Japan). A standard curve of glucose was used for the estimation of total soluble sugar.

Total soluble proteins

The Lowry (1951) technique was followed to analyze the soluble proteins in the samples. Briefly, fresh leaves were chopped in 5 mL of potassium phosphate buffer (pH 7.8) in an ice-chilled pestle and mortar. After keeping the internal temperature (4 °C) constant at 12,000 rpm, the extract was centrifuged in an ultracentrifuge machine. 100 mL of extract and 5 mL of Bradford reagent were well combined before being vortexed for 10 s. Sample absorbance was measured using a UV–visible spectrophotometer (Hitachi 220, Japan) operating at 595 nm wavelength.

Free amino acids determination

The total free amino acid was determined using the Moore and Stein method (1948). About 1 g of fresh leaf material was extracted in 10 ml of citrate buffer (pH 5.0) for 60 min at room temperature incubation. 1 ml of the sample was transferred to test tubes after centrifugation, and 1 ml of ninhydrin was then added. Aluminum foil was placed over the test tubes, which were then heated in a water bath for 30 min. The reaction was terminated in an ice bath. The sample was diluted in a 1:1 ratio with 5 ml of n-propanol and water. The sample optical density was measured at 530 nm on UV-visible spectrophotometer (Hitachi 220, Japan).

Chlorophyll content

Chlorophylls *a* and *b* were determined according to the method of Arnon (1949), and for carotenoids a method of Wellburn (1994) was followed. Briefly, fresh plant material was grounded in 80% acetone in a mortar and pestle. The crude extract was kept overnight in dark at 4 °C. Then centrifugation of extracts was done at 3000 rpm for 5 min. The optical density of the supernatant was measured spectrophotometrically at 480 nm, 645 nm, and 663 nm using 80% acetone as blank control. The values were expressed as mg g^{-1} dry matter. The chlorophyll concentrations were estimated as; Chlorophyll (*a* & *b*) (mg. g^{-1}) = $(8.02 \times A_{663} + 20.20 \times A_{645}) \times V/1000 \times W$; where V = Volume of extract (ml) and W = Weight of the leaf tissue (g). Carotenoid content = $A_{480} + (0.114 \times A_{663} - 0.638 \times A_{645})$.

Plant ionic content

To determine the tissue ionic content of plants, dried ground plant material (leaves and roots) was digested in concentrated H_2SO_4 following Wolf (1982). Cations (Na^+, K^+ and Ca^{2+}) were estimated with a flame photometer (Model 410, Sherwood Scientific Ltd., Cambridge, UK).

Statistical analysis

The data were subjected to analysis of variance (ANOVA) followed by a Tukey's pairwise comparison between different habitats at the significance level ($p > 0.05$) (Minitab 19, LLC, State College, PA, USA). Data were also subjected to multivariate analysis for principle component anlaysis (ggbiplot) and correlation matrix (ggplot2, corrplot) in R statistical software (version 4.3.1) to identify the variation and correlation between studied parameters. The study area was analyzed fro map construction using R function ggspatial in Rstudio. The data were represented graphically by using Origin Pro (version 9.1).

Results

Plant morphological attributes

Shoot length ($P < 0.05$) significantly increased in KG population from semi-arid zones followed by GW, while in extreme aridity shoot length decreased as in QN and CApopulations (Fig. 2a, Table 3). The populations from extreme arid zone showed a remarkable increase in root length as in DF populations (Fig. 2b). The population from arid regions showed a reduction in shoot fresh as compared to semi-arid where GW population showed maximum shoot fresh weight (Fig. 2c). Root fresh weight ($P < 0.05$) was significantly higher in DF population from the arid region while the semi-arid population showed a decline in root fresh weight (Fig. 2d). In semi-arid regious, shoot dry weight was maximum in GW population while in arid region it was maximum in CA population (Fig. 2e). The DF and QN populations showed maximum root dry weight as compared to other populations (Fig. 2f).

Root anatomy

Root anatomical characteristics i.e. root epidermis thickness, cortical cell, and aerenchyma area showed variable responses to aridity. Epidermis thickness was maximum in QN and DF populations from arid regions while semi-arid populations showed a decline in epidermis thickness (Fig. 3a). The cortical cell area significantly differed between the extreme and semi-arid zones (Fig. 3b). The largest cortical cell area was found in the DF and QN populations from arid conditions, whereas the GW population from a semi-arid region had the minimum values. In populations from arid regions, the area of root phloem cells continuously decreased, whereas populations KG and SG from semi-arid zones exhibited an increase in phloem area (Fig. 3c). The metaxylem area gradually increased as aridity increased, reaching a maximum in the SA population, followed by the QN population, and a minimum in the HR population from

Table 3 Morphological and anatomical characteristics of *C. ciliaris* inhabiting in different arid and semiarid habitats. Values are presented in means ± standard error

	Semi-arid								Arid							
	HR	KG	HT	KT	SG	GW	*F value*	*P* value	SA	CA	DA	HP	DF	QN	*F value*	*P* value
Morphology																
SL	30.10 ± 0.68^{b}	47.03 ± 0.79^{a}	34.26 ± 0.4^{b}	34.3 ± 0.46^{c}	25.33 ± 0.4^{ab}	39.23 ±	247.2	0.012	24.71 ± 0.71^{a}	17.01 ± 0.5^{b}	20 ± 0.57^{ab}	17.66 ± 0.6^{b}	10 ± 0.57^{c}	14 ± 0.57^{b}	144.2	0.000
RL	7.23 ± 0.2^{a}	6.46 ± 0.2^{ab}	4.66 ± 0.42^{c}	5.7 ± 0.21^{b}	6.13 ± 0.2^{ab}	4 ± 0.25^{c}	21.4	0.000	10.23 ± 0.4^{ab}	7.53 ± 0.54^{c}	10.2 ± 0.4^{ab}	12.13 ± 0.2^{b}	15.03 ± 0.5^{a}	12.53 ± 0.4^{b}	87.1	0.021
SFW	7.5 ± 0.23^{ab}	5.7 ± 0.32^{b}	11 ± 0.26^{a}	8.76 ± 0.28^{ab}	5.93 ± 0.2^{b}	11.1 ± 0.41^{a}	154.4	0.000	6.5 ± 0.23^{a}	6.46 ± 0.17^{a}	5.7 ± 0.25^{ab}	5.93 ± 0.1^{b}	4.8 ± 0.17^{b}	4.5 ± 0.15^{b}	133.9	0.011
RFW	3.6 ± 0.05 ^{b}	1.4 ± 0.05^{c}	3.76 ± 0.03^{b}	1.4 ± 0.05^{c}	2.53 ± 0.03 ^{bc}	7.33 ± 0.12^{a}	247.2	0.002	3.6 ± 0.03^{ab}	4.16 ± 0.03^{a}	3.4 ± 0.08^{ab}	2.5 ± 0.03^{b}	2.1 ± 0.03^{c}	2.4 ± 0.05^{b}	414.2	0.014
SDW	1.06 ± 0.08 ^{c}	1.16 ± 0.23^{c}	2.9 ± 0.11^{a}	1.8 ± 0.47 ^{bc}	1.16 ± 0.13^{c}	1.73 ± 0.23^{b}	131	0.001	2.66 ± 0.08^{bc}	3.5 ± 0.26^{b}	2.1 ± 0.05^{c}	3.96 ± 0.033^{bc}	4.76 ± 0.08^{a}	4.3 ± 0.11^{ab}	99	0.001
RDW	1.27 ± 0.05^{d}	0.76 ± 0.05^{c}	1.84 ± 0.05^{b}	0.53 ± 0.08 ^{c}	0.56 ± 0.005^{c}	2.79 ± 0.09^{a}	13	0.001	1.57 ± 0.05^{d}	2.62 ± 0.05^{c}	0.64 ± 0.08^{d}	2.56 ± 0.05^{c}	5.3 ± 0.15^{a}	4.03 ± 0.23^{b}	87	0.012
Root anatomy																
ET	47.23 ± 2.3 ^{a}	33.06 ± 2.3^{b}	47.23 ± 2.3 ^{a}	47.23 ± 2.3 ^{a}	33.06 ± 2.5 ^{b}	42.51 ± 2.3 ^{ab}	12.32	0.041	75.57 ± 4.2 ^{ab}	56.68 ± 2.8^{c}	70.85 ± 4.7^{b}	75.59 ± 3.5 ^{ab}	90.29 ± 4.2^{a}	81.55 ± 3.1 ^{ab}	44.20	0.014
CCA	2313.85 ± 157.7 ^{ab}	2050.9 ± 157.7 ^{b}	2261.2 ± 420.7^{b}	2892.3 ± 449.3^{a}	2050.9 ± 145.21^{b}	1419.8 ± 189.6^{c}	21.4	0.033	2050.9 ± 258.4^{c}	2734.5 ± 157.7^{c}	2313.8 ± 241.4^{c}	1893.152 ± 165.2^{d}	7677.7 ± 422.6^{a}	4680.2 ± 402.6^{b}	47.1	0.010
PA	736.2 ± 61.2^{b}	1104.3 ± 80.4^{a}	841.4 ± 70.8^{ab}	578.4 ± 59.6^{bc}	1104.3 ± 42.5^{a}	315.5 ± 52.4^{c}	124.4	0.001	631.05 ± 72.16^{a}	631.05 ± 72.16 ^{a}	578.4 ± 50.4^{ab}	368.1 ± 42.5^{b}	315.5 ± 42^{b}	525.8 ± 52.3^{ab}	113.9	0.029
MA	1998.3 ± 631.1^{c}	3155.2 ± 631.1^{b}	4627.7 ± 567.1^{a}	4522.5 ± 567^{a}	3155.2 ± 415.1^{b}	2839.7 ± 556^{b}	261.2	0.000	11,884.7 ± 517.9^{a}	3733.7 ± 647.7^{c}	2156.09 ± 667.9^{d}	5100.9 ± 515.6^{c}	9728.7 ± 831.5^{b}	11,043.3 ± 814.1^{ab}	414.2	0.000
MA	2681.9a ± 157.6	1525.0c ± 57.9	1209.5d ± 82.1	2103.50b ± 111.3	1525.03c ± 136.7	1419.8 cd ± 47.92	146.2	0.024	971.61ab ± 73.6	1162.1a 63.1	893.1ab ± 112	1076.7a ± 136.7	631.05b ± 60.5	262.9c ± 50.5	251	0.000
PCA	2313.8 ± 120.7^{ab}	1577.6 ± 182.1^{b}	2261.2 ± 189.6^{ab}	2647.1 ± 384.5^{a}	1577.6 ± 112^{b}	1315 ± 182.1^{c}	9.25	0.043	3838.8 ± 346.3^{bc}	1419.8 ± 113.2^{d}	1682.8 ± 210.3^{d}	2331.6 ± 412^{c}	7459.07 ± 426.5^{a}	6836.3 ± 408.3^{b}	98	0.001
Stem anatomy																
CCA	3470.77 ± 189.6^{b}	1525.03 ± 268.8^{c}	4995.8 ± 278.2^{ab}	2208.6 ± 234.8 ^{bc}	1367.2 ± 219.7^{c}	6152.7 ± 218.3^{a}	116.2	0.000	3155.2 ± 229.2^{a}	2787.1 ± 229.1^{a}	1945.7 ± 331^{ab}	1209.5 ± 182.1^{b}	161.1 ± 88.2^{c}	631.0 ± 139.1 ^{bc}	84.2	0.001
MA	6468.27 ± 385.6^{b}	1682.8 ± 210.3^{cd}	1051.7 ± 338.2^{d}	2103.5 ± 260.5^{c}	1735.3 ± 317.4^{cd}	8466.5 ± 358.4^{a}	91.4	0.021	1472.4 ± 360.8^{ab}	1104.3 ± 157.7^{ab}	1262.1 ± 315.5^{ab}	2103.5 ± 356.5^{a}	683.6 ± 139.1^{b}	2313.8 ± 139.1^{a}	74.1	0.025
PA	522.5 ± 23.3^{ab}	631.05 ± 17.8^{a}	449.2 ± 24.1^{b}	315.5 ± 31.7^{c}	525.8 ± 34.2^{ab}	510.9 ± 26.5^{ab}	114.4	0.013	315.5 ± 17.8^{b}	493.9 ± 17.52^{a}	219.8 ± 23.9^{d}	241.4 ± 17.39^{c}	368.1 ± 15.4^{ab}	262.9 ± 15.4^{c}	97.9	0.027
VBA	24,558.3 ± 1138.8^{a}	15,513.3 ± 912.3^{b}	21,508.3 ± 1689^{ab}	12,305.4 ± 1504.4^{c}	15,145.2 ± 1252.2^{b}	14,671.9 ± 847.7^{b}	251.2	0.004	15,828.8 ± 824.7^{b}	5837.2 ± 1091.1^{e}	10,675.2 ± 702.5^{c}	18,510.8 ± 793.2^{a}	3523.3 ± 763.5^{f}	9833.8 ± 1056.1^{d}	314.2	0.002
Leaf blade anatomy																
LT	94.4 ± 9.0^{b}	80.2 ± 7^{bc}	94.4 ± 9.6^{b}	113.3 ± 8.1^{ab}	155.8 ± 10.2^{a}	70.8 ± 8.1^{c}	51.32	0.009	146.4 ± 9.4 ^{bc}	99.1 ± 9.3^{c}	113.3 ± 8.18^{c}	155.1 ± 9.7^{b}	184.2 ± 8.1^{a}	165.3 ± 10.7^{ab}	124.2	0.000

Table 3 (continued)

	Semi-arid								Arid							
	HR	KG	HT	KT	SG	GW	*F value*	*P* value	SA	CA	DA	HP	DF	QN	*F value*	*P* value
MT	220.6a ± 17.03	179.4a ± 12.4	250.1a ± 21.6	200.2a ± 8.1	136.9b ± 9.4	193.6ab ± 9.4	±71.4	0.031	316.4a ± 12.4	250.3b ± 12.4	240.8b ± 21.6	170.04c ± 18.5	132.2d ± 12.4	141.7d ± 8.1	±107	0.013
PA	473.2 ± 17.03^{c}	420.7 ± 12.4^{c}	946.5 ± 21.6^{a}	683.6 ± 8.1^{b}	838.8 ± 9.4^{ab}	578.4 ± 9.4 ^{bc}	±104.4	0.014	683.6 ± 12.4 ^{bc}	578.4 ± 12.4^{c}	631.05 ± 21.6^{c}	762.10 ± 24.5^{b}	930.3 ± 22.4^{a}	836.3 ± 15.1^{ab}	±93.9	0.003
MA	4943.2 ± 347.2^{b}	1051.7 ± 65.4^{d}	6305.4 ± 237.6^{a}	1577.6 ± 26^{c}	1841.4 ± 15.02^{c}	5302.9 ± 358.2^{ab}	±131.2	0.001	1999.1 ± 149.2^{b}	2629.3 ± 218.2^{a}	2473.2 ± 113.01^{ab}	999.1 ± 171.6 ^{bc}	683.6 ± 119.8^{c}	1998.3 ± 251.7^{ab}	±114.2	0.004
ET	2232.1 ± 304^{d}	2863.2 ± 218 ^{bc}	2456.3 ± 241^{c}	3542.1 ± 324^{a}	3054.3 ± 300^{b}	2550.3 ± 311^{c}	±96.0	0.021	3832.1 ± 324^{d}	4456.2 ± 307.1^{c}	4023.2 ± 344^{cd}	4523.1 ± 348 ^{bc}	7845.1 ± 378^{a}	6123.1 ± 358^{b}	±151	0.001
BA	34 ± 0.64^{c}	50 ± 0.96^{a}	40 ± 0.63^{b}	48 ± 0.85^{a}	41 ± 0.62^{b}	44 ± 0.7^{b}	22	0.001	64 ± 0.8^{c}	60 ± 0.63^{d}	71 ± 0.89^{c}	77 ± 0.99^{b}	80 ± 1.1^{ab}	85 ± 1.3^{a}	91	0.021
Leaf epidermal anatomy																
AbSD	23.6 ± 1.15^{a}	17 ± 1.02^{b}	20.3 ± 1.2^{ab}	17 ± 0.5^{b}	16.6 ± 0.7^{b}	19.6 ± 0.8^{ab}	±96.2	0.012	17.3 ± 0.8^{a}	11.6 ± 0.8^{b}	14.3 ± 0.9^{ab}	10.6 ± 0.7^{c}	8 ± 0.6^{d}	8.3 ± 0.6^{d}	184.2	0.001
AbSA	10,716.1 ± 247.5^{a}	7362.2 ± 133.7^{b}	9873.08 ± 253.5^{ab}	3050.07 ± 105.1^{c}	7572.60 ± 244.5^{b}	9671.09 ± 321.01^{ab}	±81.4	0.031	4207.0 ± 267.5^{ab}	5732.04 ± 267.4^{a}	4364.7 ± 178.4^{ab}	3260.4 ± 118.4^{b}	2630.2 ± 109.9^{c}	3365.6 ± 188.7^{b}	±94.1	0.021
AdSD	23.6 ± 1.08^{a}	17 ± 1.08^{b}	20.33 ± 1.2^{ab}	17 ± 0.8^{b}	16.66 ± 1.02^{b}	19.6 ± 1.4^{ab}	±114.4	0.011	17.3 ± 0.6^{a}	11.67 ± 1.05^{b}	14.3 ± 0.7^{ab}	10.66 ± 0.7^{b}	8 ± 0.3^{c}	8.3 ± 0.5^{c}	97.9	0.014
AdSA	10,675.27^{x} ± 376.2^{c}	5442.8 ± 256.3^{ab}	10,359.7 ± 325.9^{a}	3102.66 ± 130.4^{c}	4627.70 ± 125.4^{b}	2734.5 ± 320.7^{c}	±151.2	0.001	5258.75 ± 320.7^{a}	5732.04 ± 243.3^{a}	2944.90 ± 256.5^{b}	3996.65 ± 152.4^{ab}	2839.7 ± 146.5^{b}	2313.8 ± 220.7^{c}	±141.2	0.015

Sites: *KG* Kanhati Mountains; *KT* Katha, SG Sargodha; *HR* Head Rasul; *GW* Gutwala; *SA* Salmani Adda; *HT* Head Trimu; *CA* Chock Azam; *DA* Darbar Anayat Shah; *QN* Qila Nawabdin; *DF* Derawer Fort; *HP* Hasilpur Morphology: *SL* shoot length; *RL* root length; *SFW* shoot fresh weight; *RFW* root fresh weight; *SDW* shoot dry weight; *RDW* root dry weight Root anatomy: *ET* epidermal thickness; *CCA* cortical cell area; *PA* phloem area; *MA* metaxylem area; *PCA* pith cell area; *AA* aerenchyma area Stem anatomy; *CCA* cortical cell area; *MA* metaxylem area; *PA* phloem area; *VBA* vascular bundle area Leaf blade anatomy; *LT* lamina thickness; *MT* midrib thickness; *PA* phloem area; *MA* metaxylem area; *ET* epidermal thickness; *BA* bulliform area Leaf epidermal anatomy; *AbSD* abaxial stomatal density; *AbSA* abaxial stomatal area; *AdSD* adaxial stomatal density; *AdSA* adaxial stomatal area

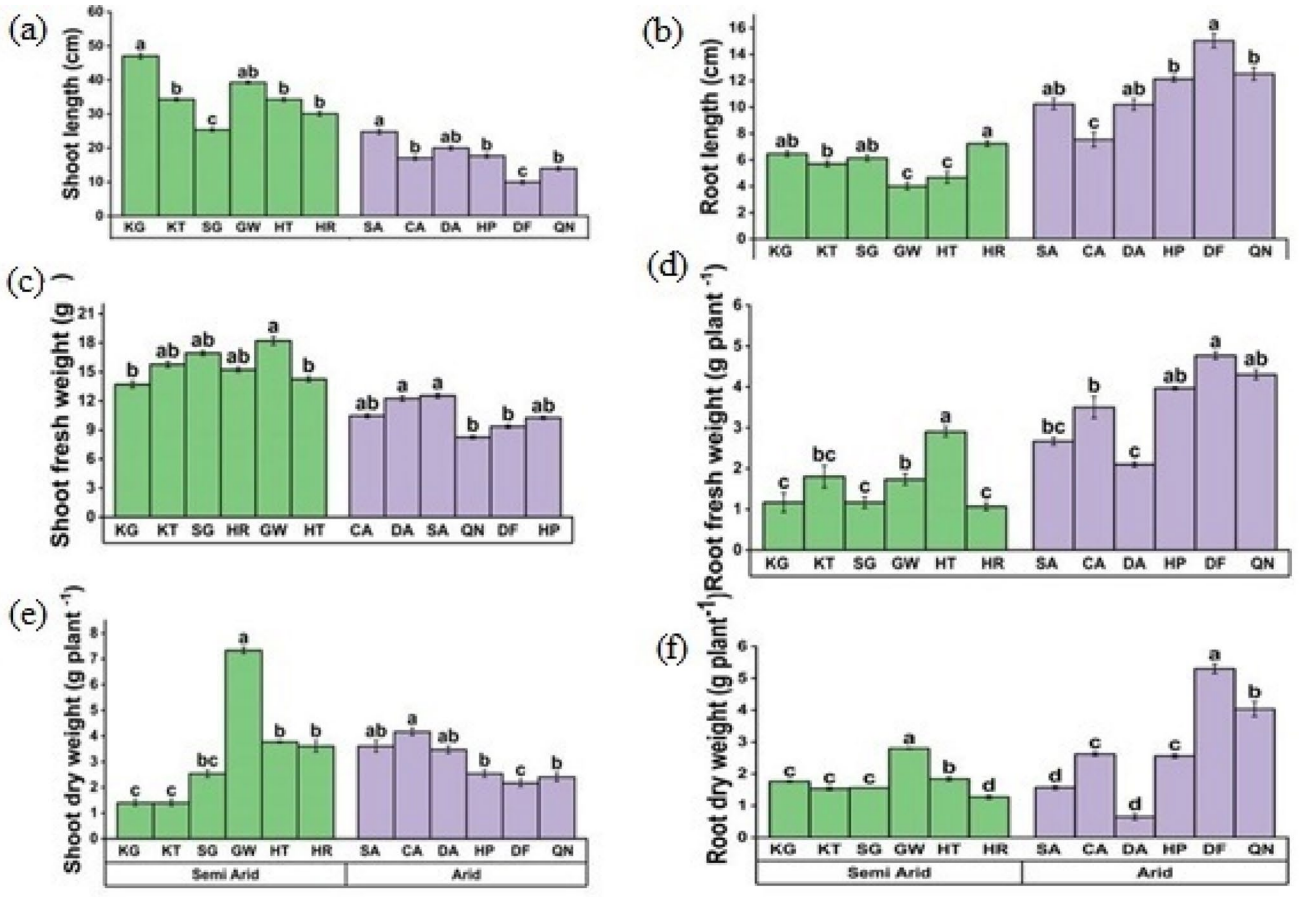

Fig. 2 Morphological attributes **a** Shoot length **b** Root length **c** Shoot fresh weight **d** Root fresh weight **e** Shoot dry weight **f** Root dry weight of *C. ciliaris* collected from different arid and semi- arid zones of Punjab. Bars represent mean and standard error. Means with different letters are significant at $p > 0.05$

the semi-arid zone (Fig. 3d). Pith cell area was maximum in the HR and KT populations and decreased with increasing aridity, whereas it was lowest in the QN population (Fig. 3e). The Aerenchyma area gradually increased in populations from arid zones, as seen in DF and QN populations, whereas it gradually declined in populations from less dry environments, reaching its lowest level in GW and SG populations (Fig. 3f).

Stem anatomy

Stem anatomical features of *C. ciliaris* varied significantly from semi-arid to arid climates. DF populations from arid regions exhibited significantly reduced cortical cell area while GW and HT populations from semi-arid zone showed maximum cortical cell area (Fig. 4a). All populations dwelling in arid regions had a decrease in metaxylem area, with DF and CA populations having the lowest values (Fig. 4b). A lower value of phloem cell area was observed in the CA population, followed by the QN population from an arid zone (Fig. 4c). In semi-arid regions, was maximal in HT and GW populations, followed by the HR population of the semi-arid zone. The vascular bundle area showed variation from semi-arid to arid zones. HR population showed maximum vascular bundle area followed by HT population in the semi-arid zone while it was minimum in the DF and CA population of the arid zone (Fig. 4d).

Leaf blade anatomy

C. ciliaris populations from both arid and semi-arid zones showed significant variations in leaf anatomical structure. Lamina thickness increased along with an increase in water scarcity. Maximum values of lamina thickness were observed in the QN and DF populations, while minimal values were observed in the semi-arid populations' GW and KG (Fig. 5a). The DF and QN populations from the arid zone had thick midribs, whereas the SG population from the semi-arid zone had reduced midrib thickness (Fig. 5b).

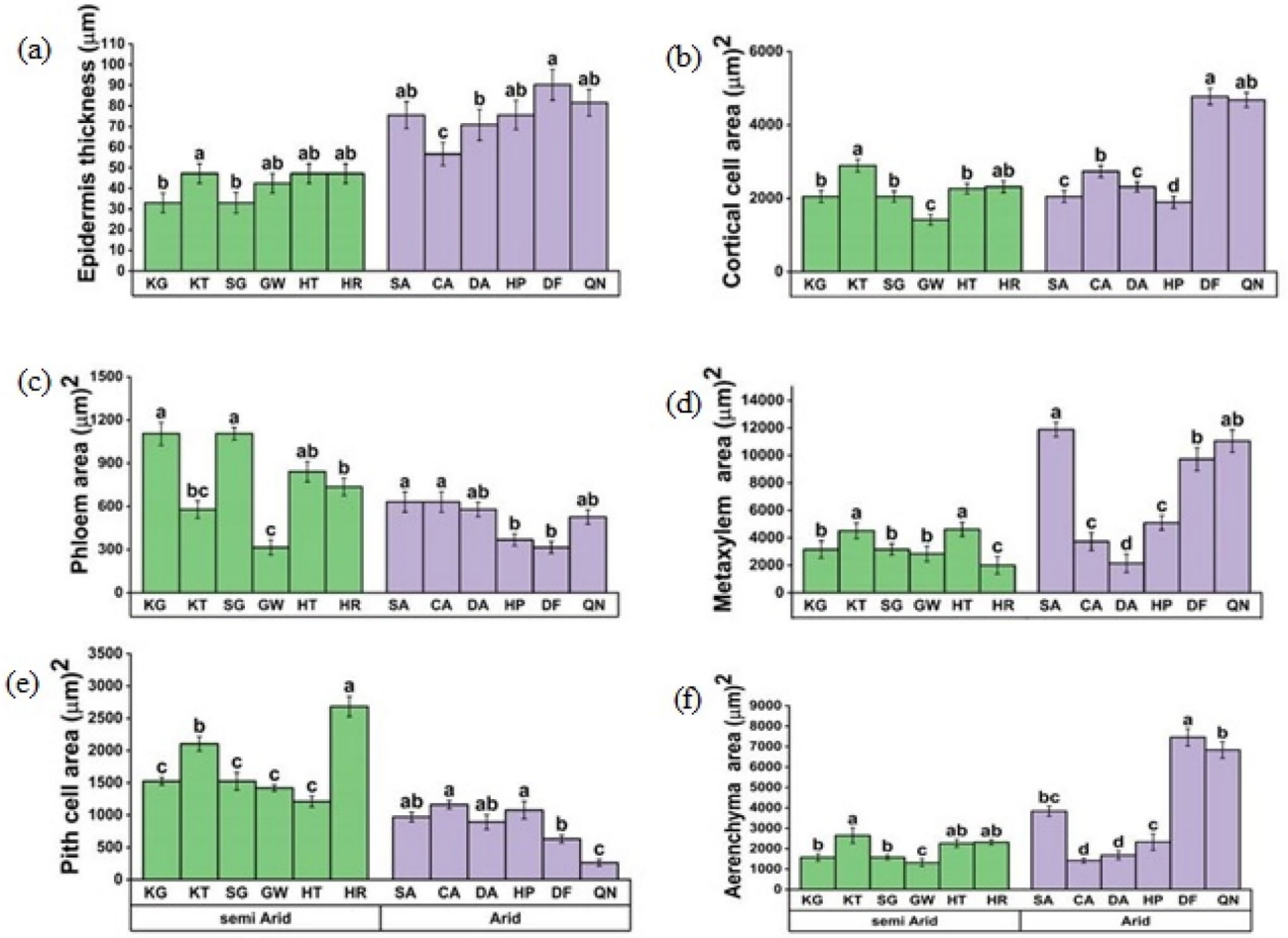

Fig. 3 Root anatomical characteristics **a** Epidermal thickness **b** Cortical cell area **c** Phloem area **d** metaxylem area **e** Pith cell area **f** Aerenchyma area of *C. ciliaris* from different arid and semi- arid zones of Punjab. Bars represent mean and standard error. Means with different letters are significant at $p > 0.05$

A significant increase ($P < 0.05$) in the phloem area was more obvious in the HT population from the semi-arid zone followed by the SG population (Fig. 5c). All populations from the arid region demonstrated a consistent decline in metaxylem area, while the DF and KG populations from the semi-arid area showed the lowest metaxylem area. HT population showed a maximum increase in the metaxylem area (Fig. 5d). Epidermal thick was significantly higher in arid populations compared to semi-arid populations (Fig. 5e). In arid populations, DF and QN showed substantial increase in bulliform cell area (Fig. 5f).

Leaf epidermal anatomy

In comparison to populations from arid regions, semiarid populations had significantly higher stomatal density and area on the abaxial and adaxial sides of the leaves (Fig. S4, Fig. S5). The maximum number of stomata on the abaxial and adaxial surface was recorded in the HR population from the semi-arid zone while QN and DF populations from the arid zone had minimum abaxial and adaxial stomatal density (Figs. 6a, c). The abaxial stomatal area was maximum in the semi-arid HR population followed by HT and GW population and its minimum was recorded in the KT population. In an arid climate, the CA population had the maximum abaxial stomatal area while the minimum was observed in the DF population. A larger adaxial stomatal area was observed in HT and HR populations and a smaller area was recorded in QN populations from the arid zone (Figs. 6b,d).

Organic osmolytes

Organic osmolytes changed substantially ($P < 0.05$) in C. *ciliaris* populations from arid to semi-arid zones (Table 4). The maximum concentration of glycine betaine was recorded in the arid zone population QN and its minimum value was recorded in the semi-arid population HR (Fig. 7a).

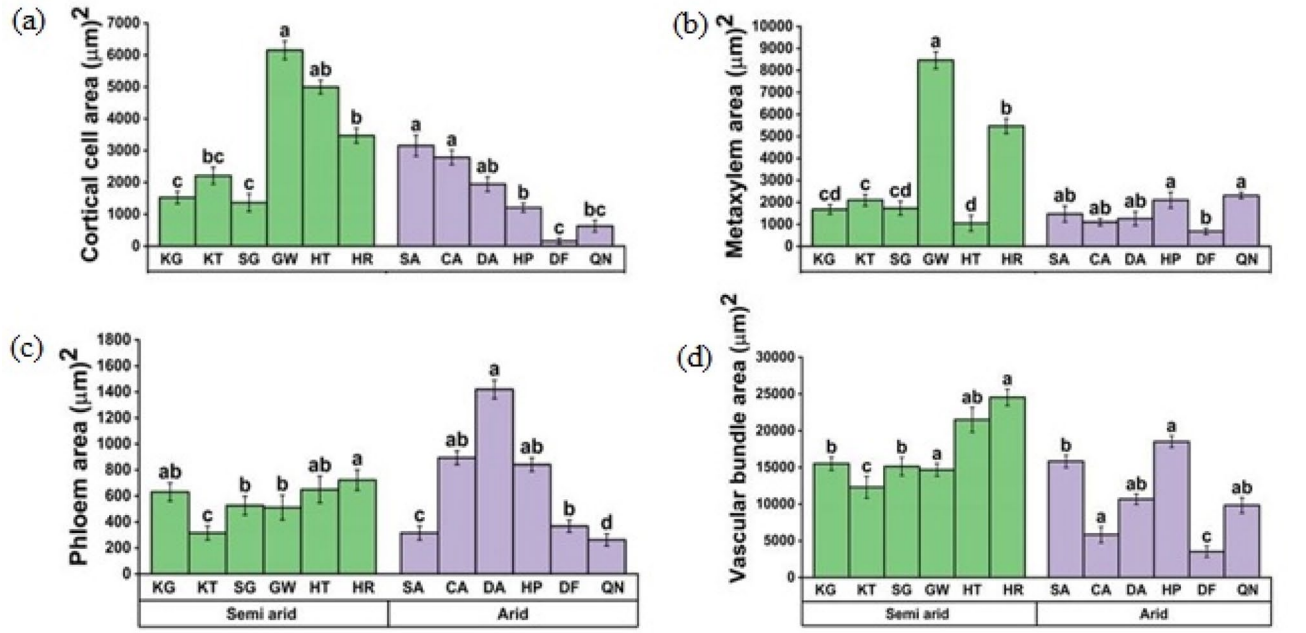

Fig. 4 Stem anatomical attributes **a** Cortical cell area **b** Metaxylem area **c** Phloem area **d** Vascular bundle area of *C. ciliaris* from different arid and semi-arid zones of Punjab. Bars represent mean and standard error. Means with different letters are significant at $p > 0.05$

The proline concentration was maximum in the DF population from the arid zone while the minimum GW from semi-arid population (Fig. 7b). The concentration of total soluble sugars was highest in the HT population from the semi-arid zone while its lowest concentration was in CA and DF populations from arid regions (Fig. 7c). Total soluble proteins decreased in arid populations, its minimum value was found in QN populations while semi-arid region GW and SG populations showed a substantial increase in this parameter (Fig. 7d). The free amino acid concentration was maximum in the DF and HP populations collected from the arid zone and semi-arid populations i.e., HR and KT populations showed lower values of total amino acids (Fig. 7e). The concentration of chlorophyll *a* was observed maximum in the GW population from semi-arid and its value was minimum in the QN population from the arid zone (Fig. 7f). HR population collected from the semi-arid region showed the highest concentration of chlorophyll *b* and less concentration was observed in the HP population from the arid climatic zone (Fig. 7g). Total carotenoid contents were decreased in the DF population collected from the arid zone (Fig. 7h).

Ionic contents

The maximum concentration of Na was in the root and shoot of the QN population from the arid zone while root Na and shoot Na was the minimum in HT and GW populations respectively from the semi-arid zone (Fig. 8a). The maximum root K was in the GW population and its minimum was recorded in the DF population. SG population from the semi-arid zone showed maximum shoot K concentration and its minimum value was recorded in the QN population from the arid zone (Fig. 8b). The root of the DF population showed the highest Ca contents, and the least concentration was recorded in the KT population from the semi-arid zone (Fig. 8c).

Multivariate analysis

Correlation matrix

The attributes studied under aridity showed a significant correlation ($P < 0.05$). The shoot fresh weight with stem cortical cell area, root fresh weight with root cortical cell area, shoot fresh weight with leaf metaxylem area, and shoot length with abaxial stomatal density had a positive correlation. There was a negative correlation between root fresh weight with pith cell area, shoot length with leaf thickness, root fresh weight with the adaxial stomatal area, pith cell area, and glycinebetaine with shoot K (Fig. 9a). Glycine betaine with the shoot and root Na, proline, and free amino acid with root Ca had a strong positive correlation (Fig. 9b).

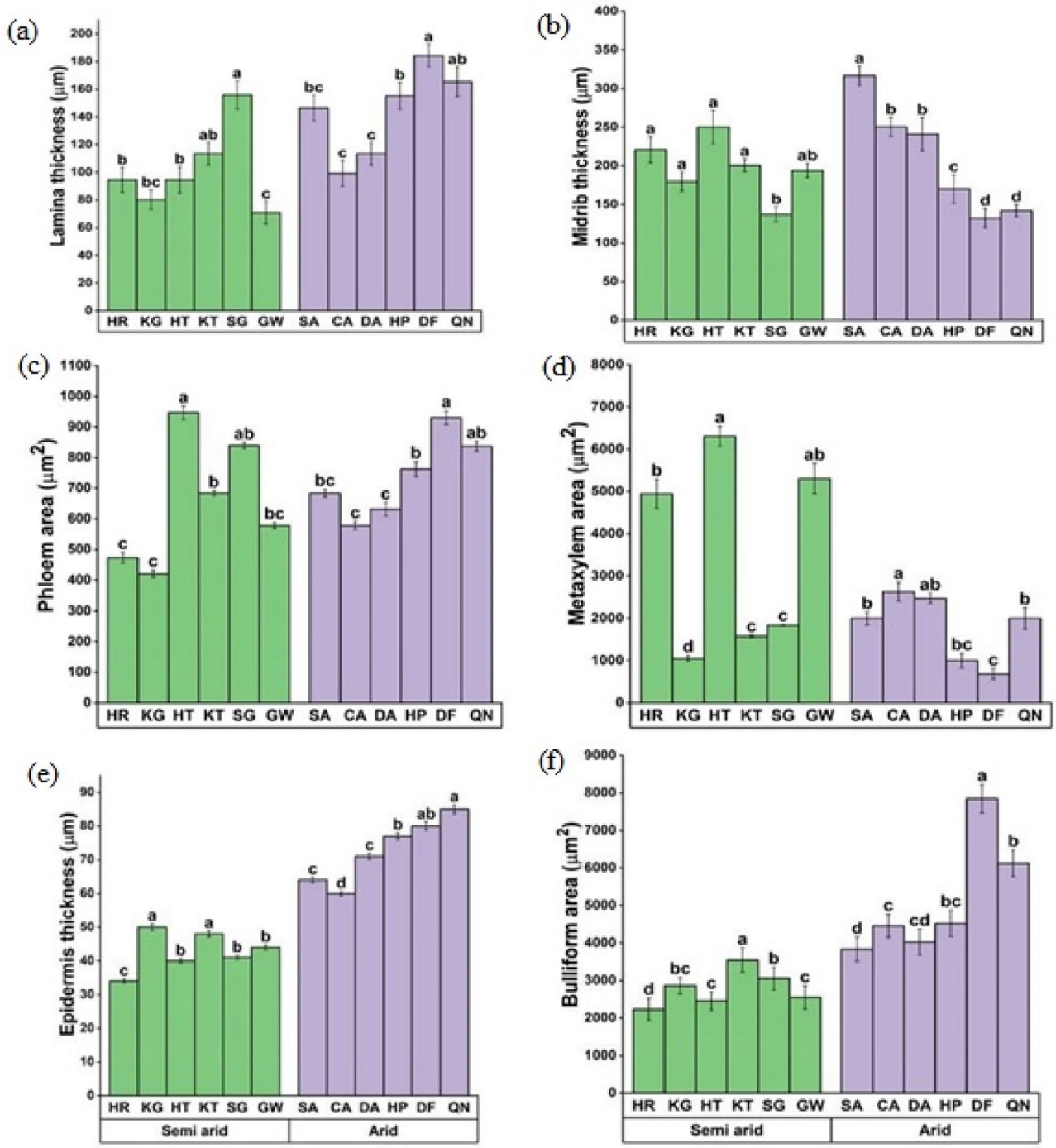

Fig. 5 Leaf blade anatomical attributes **a** Lamina thickness **b** Midrib thickness **c** Phloem area **d** Metaxylem area **e** Epidermal thickness **f** Bulliform area of *C. ciliaris* from different arid and semi-arid zones of Punjab. Bars represent mean and standard error. Means with different letters are significant at $p > 0.05$

Principle components analysis (PCA)

The principal components analysis showed significant effects ($P < 0.05$) of aridity on the growth and anatomy of *C. ciliaris*. The contribution of Dim1 to total variance was (49.5%) in comparison to Dim2 which showed (16.2%) variation out of a total 65.7% variation in the dataset (Fig. 10a). The major contributors to semi-arid environment were pith cell area, abaxial and adaxial stomatal density, abaxial stomatal area, stem phloem area, shoot length, leaf metaxylem

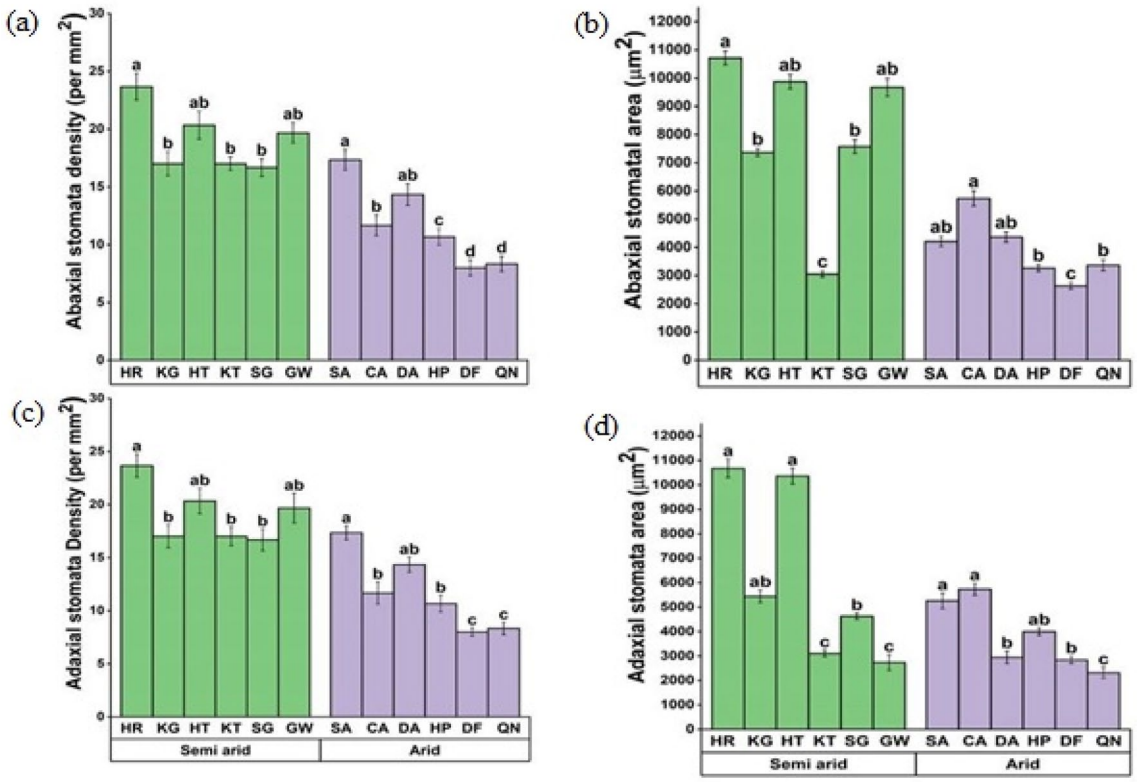

Fig. 6 Leaf epidermal anatomy **a** Abaxial stomatal density **b** Abaxial stomatal area **c** Adaxial stomatal density **d** Adaxial stomatal area of *C. ciliaris* from different arid and semi-arid zones of Punjab. Bars represent mean and standard error. Means with different letters are significant at $p > 0.05$

area, root and stem phloem area, midrib thickness and shoot dry weight. Principal contributors to arid environment were root fresh and dry weight, root cortical cell area, root metaxylem area, leaf lamina thickness, root epidermal thickness, and root aerenchyma area. Root length and root dry weight showed negative values (− 1) and higher positive (+ 3) eigenvalues respectively. The second PCA is constructed for growth, physiology, and root and shoot ionic contents. Of the total variation Dim 1 contributed 62.7% in contrast with Dim 2 which contributed 13% (total 75.7%). Root fresh and dry weight, glycinebetaine, total soluble sugars, proline, shoot Ca, free amino acid, and root length were the principal contributors to the arid climate. The major contributors to the semi-arid climate were shoot fresh weight, shoot length, total soluble protein, root Na, and root K. Shoot dry weight and shoot K showed higher positive (+ 2) and negative (− 1) eigenvalue respectively (Fig. 10B).

Discussion

C. ciliaris is a C_4 perennial grasse (Mansoor et al. 2019) that exhibits adaptability to a variety of habitats encountering multiple stresses including drought (Mganga et al. 2023) salinity (Al-Dakheel et al. 2016). The evolutionary process has played a critical role in the development of tolerant plant ecotypes, leading to the discovery of various populations with distinct structural and functional adaptations to cope with extreme environmental conditions (Farooq et al. 2009). This study focuses on key mechanisms that mediate stress tolerance at the anatomical and physiological levels, providing deep insights into how these plants not only survive but also succeed in the face of adversity in their environments.

The most adverse impact of environmental stresses like salinity and drought is related to water scarcity, and therefore conservation of water is the utmost requirement of a plant species for successful survival (Zhang et al. 2023). Water conservation is crucial for plants growing in arid climates (Iqbal et al. 2022). Preventing water loss via the plant surface 3 can be accomplished by thick epidermis and cuticle,

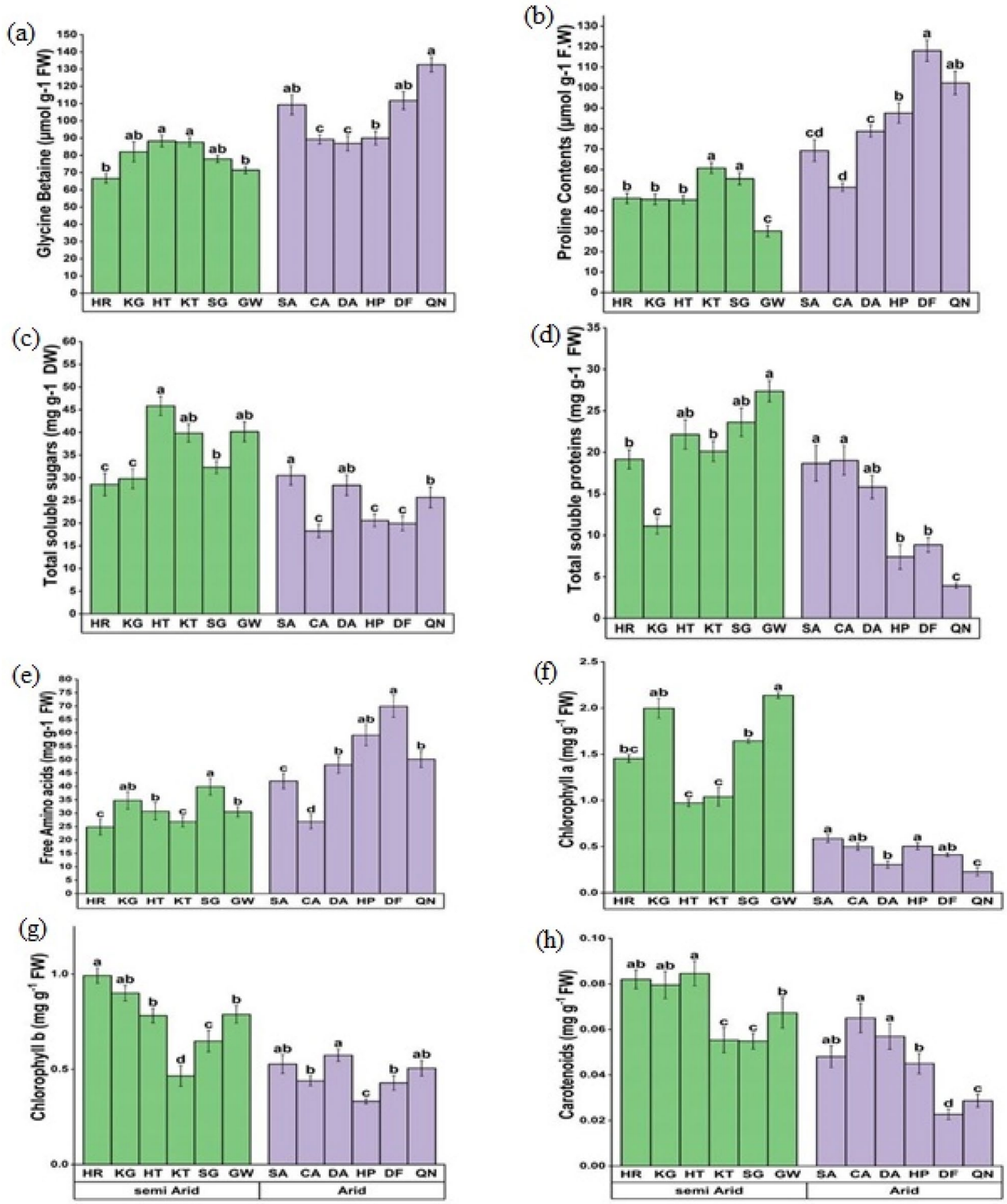

Fig. 7 Organic osmolytes **a** Glycine betaine **b** Proline content **c** Total soluble sugars **d** Total soluble proteins **e** Free amino acids and **f** Chlorophyll *a* **g** Chlorophyll *b* **h** Carotenoids of *C. ciliaris* collected from different arid and semi-arid zones of Punjab. Bars represent mean and standard error. Means with different letters are significant at $p > 0.05$

Table 4 Photosynthetic pigments, organic osmolytes and plant ionic contents of *C. ciliaris* inhabiting in different arid and semi-arid habitats. Values are presented in means ± standard error

	Semi-arid								Arid							
	HR	KG	HT	KT	SG	GW	*F value*	*P* value	SA	CA	DA	HP	DF	QN	*F value*	*P* value
Photosynthetic pigments																
Chlorophyll *a*	1.45 ± 0.04 ^{bc}	1.99 ± 0.10^{ab}	0.97 ± 0.03^{c}	1.03 ± 0.09^{c}	1.64 ± 0.02^{b}	2.13 ± 0.03^{a}	132.0	0.000	0.58 ± 0.03^{a}	0.49 ± 0.03^{ab}	0.30 ± 0.03^{b}	0.50 ± 0.03^{a}	0.41 ± 0.02^{ab}	0.22 ± 0.04^{c}	116.1	0.001
Chlorophyll *b*	0.99 ± 0.04^{a}	0.89 ± 0.04^{ab}	0.78 ± 0.03^{b}	0.46 ± 0.05^{d}	0.64 ± 0.05^{c}	0.78 ± 0.04^{b}	165.1	0.000	0.52 ± 0.04^{ab}	0.43 ± 0.02^{b}	0.57 ± 0.03^{a}	0.33 ± 0.01^{c}	0.42 ± 0.03^{b}	0.50 ± 0.04^{ab}	103.5	0.001
Carotenoid	0.07 ± 0.005^{c}	0.05 ± 0.005^{c}	0.054 ± 0.003^{d}	0.067 ± 0.006^{b}	0.08 ± 0.005^{a}	0.08 ± 0.004^{a}	201.1	0.000	0.04 ± 0.004^{ab}	0.065 ± 0.006^{c}	0.056 ± 0.005^{a}	0.045 ± 0.004^{b}	0.022 ± 0.002^{d}	0.028 ± 0.002^{c}	138.1	0.002
Organic osmolytes																
Glycine betaine	66.51 ± 2.6^{b}	82 ± 5.7^{ab}	88.27 ± 3.3^{a}	87.60 ± 2.6^{a}	77.82 ± 2.0^{ab}	71.4 ± 2.05^{b}	91.13	0.001	109.3 ± 5.74^{ab}	89.28 ± 2.7^{c}	86.91 ± 4.32^{c}	90 ± 4.01^{b}	111.73 ± 5.1^{ab}	132.60 ± 4.2^{a}	164.2	0.000
Proline	46.01 ± 2.5^{b}	45.49 ± 2.5^{b}	45.29 ± 1.9^{b}	60.74 ± 2.6^{a}	55.54 ± 2.9^{a}	30.04 ± 2.7^{c}	121.18	0.000	69.29 ± 5.3^{cd}	51.41 ± 2.01^{d}	78.66 ± 2.7^{c}	87.56 ± 4.9^{b}	118.01 ± 5.1^{a}	102.30 ± 5.6^{ab}	78.2	0.002
Total soluble sugars	28.50 ± 2.4^{c}	29.77 ± 2.1^{c}	45.84 ± 2.1^{a}	39.83 ± 1.9^{ab}	32.28 ± 1.3^{b}	40.14 ± 2.1^{ab}	109.73	0.001	30.50 ± 2.1^{a}	18.26 ± 1.4^{c}	28.34 ± 2.5^{ab}	20.58 ± 1.3^{c}	19.92 ± 1.5^{c}	25.68 ± 2.2^{b}	132.1	0.000
Total soluble proteins	19.15 ± 1.1^{b}	11.10 ± 0.95^{c}	22.15 ± 1.7^{ab}	20.1 ± 1.2^{b}	23.62 ± 1.6^{ab}	27.36 ± 1.2^{a}	54.21	0.0021	18.67 ± 2.1^{a}	19.02 ± 1.7^{a}	15.81 ± 1.3^{ab}	7.38 ± 1.4^{b}	8.84 ± 0.86^{b}	3.91 ± 0.28^{c}	111.21	0.001
Total free amino acids	24.82 ± 2.9^{c}	34.75 ± 3.2^{ab}	30.71 ± 3.1^{b}	26.82 ± 1.9^{c}	39.88 ± 3.1^{a}	30.52 ± 1.9^{b}	130.0	0.021	41.99 ± 2.8^{c}	26.81 ± 2.6^{d}	48.05 ± 3.1^{b}	59.15 ± 3.9^{ab}	69.90 ± 4.06^{a}	50.14 ± 3.06^{b}	122.1	0.024
Ionic contents																
Shoot Na^+	29.37 ± 0.85^{a}	22.36 ± 1.5 ^{bc}	26.94 ± 1.7^{ab}	24.46 ± 2.3^{b}	20.95 ± 1.06^{c}	26.01 ± 1.8^{ab}	211.1	0.000	39.57 ± 1.1 ^{bc}	33.66 ± 1.9^{c}	31.17 ± 1.9^{d}	51.68 ± 2.1^{a}	47.12 ± 2.82^{ab}	42.19 ± 1.73^{b}	189.1	0.001
Root Na^+	31.63 ± 1.73^{ab}	34.06 ± 1.7^{a}	30.54 ± 1.6^{b}	30.98 ± 2.2^{b}	27.54 ± 1.86^{c}	24.08 ± 1.6^{d}	179.36	0.012	40.05 ± 2.37^{c}	36.93 ± 1.9^{cd}	34.31 ± 2.4^{d}	50.32 ± 2.8^{a}	47.77 ± 2.4^{b}	34.26 ± 1.73^{d}	136.91	0.023
Shoot K^+	16.06 ± 0.65^{c}	16.56 ± 0.43^{c}	20.53 ± 0.94^{a}	17.30 ± 0.86^{b}	18.56 ± 0.43^{ab}	14.57 ± 0.65^{d}	143.01	0.002	14.32 ± 0.43^{ab}	12.56 ± 0.89^{b}	10.81 ± 0.39^{c}	5.33 ± 0.57^{cd}	8.80 ± 0.49^{d}	15.31 ± 1.08^{a}	111.31	0.031
Root K^+	17.28 ± 0.89^{c}	22.52 ± 0.43^{ab}	20.51 ± 0.65^{b}	18.28 ± 0.65^{c}	23.52 ± 0.65^{a}	20.53 ± 0.65^{ab}	98.34	0.023	15.27 ± 0.6^{ab}	12.49 ± 0.8^{b}	9.04 ± 0.6^{cd}	16.25 ± 0.43^{a}	7.02 ± 0.8^{d}	10.77 ± 0.6^{c}	112.35	0.001
Shoot Ca^{2+}	9.56 ± 1.05 ^{bc}	14.46 ± 1.2^{a}	13.31 ± 1.2^{ab}	7.26 ± 0.8^{c}	5.26 ± 0.4^{d}	11.51 ± 0.9^{b}	136.26	0.000	21.56 ± 1.3^{ab}	20.36 ± 1.2^{b}	15.86 ± 1.2^{c}	14.56 ± 1.3^{c}	22.98 ± 1.4^{a}	18.56 ± 1.5^{b}	102.3	0.001
Root Ca^{2+}	5.52 ± 0.5^{b}	4.80 ± 0.3^{c}	8.93 ± 0.5^{a}	5.90 ± 0.4^{b}	4.98 ± 0.5^{c}	7.20 ± 0.4^{ab}	121.60	0.019	6.73 ± 0.4^{d}	10.13b ± 0.49	10.65 ± 0.5^{b}	13.02 ± 0.7^{ab}	15.75 ± 0.7^{a}	8.38 ± 0.5^{c}	156.3	0.002

Sites: *KG* Kanhati Mountains; *KT* Katha; *SG* Sargodha; *HR* Head Rasul; *GW* Gutwala; *SA* Salmani Adda; *HT* Head Trimu; *CA* Chock Azam; *DA* Darbar Anayat Shah; *QN* Qila Nawabdin; *DF* Derawer Fort; *HP* Hasilpur

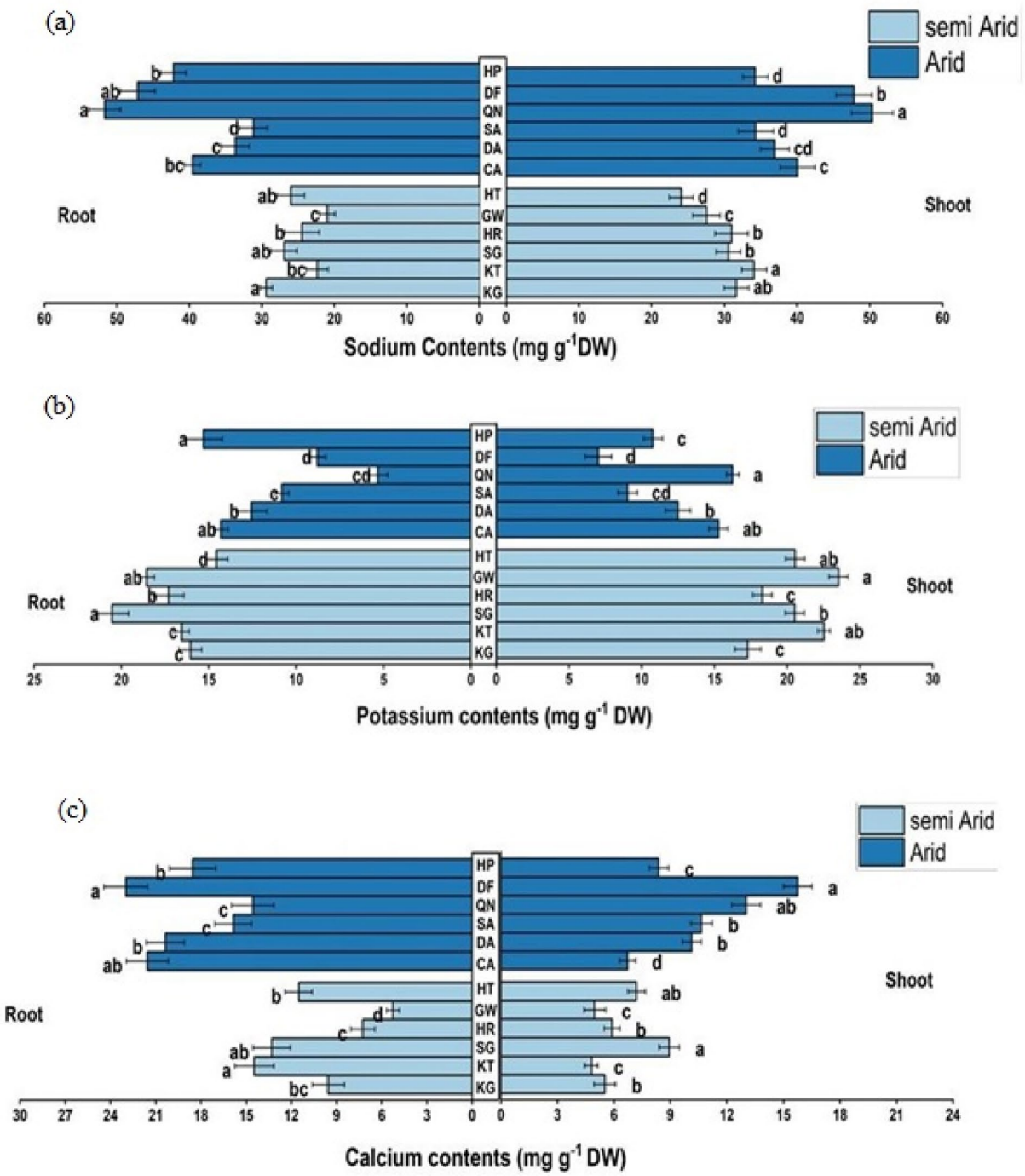

Fig. 8 Ionic contents of *C. ciliaris* from different arid and semi-arid zones of Punjab. **a** Root and shoot sodium contents **b** Root and shoot potassium contents **c** Root and shoot calcium contents. Bars represent mean and standard error. Means with different letters are significant at $p > 0.05$

high accumulation of osmoprotectants, a high proportion of dermal tissues (epidermis and stomata), storage tissues (cortex and pith) and (vascular bundles and metaxylem) tissues (Nawaz et al. 2013; Fatima et al. 2018; Waseem et al. 2021).

Biomass is a reliable indicator for assessing stress tolerance in a species. Consequently, an increase in biomass production in *C. ciliaris* shows a high degree of drought and stress tolerance. In the present study, all populations of *C. ciliaris* showed morphological differential along aridity gradient. For instance, root fresh and dry weight increased in population growing in extremely arid conditions. The increase in root biomass is an adaptive mechanism to retain

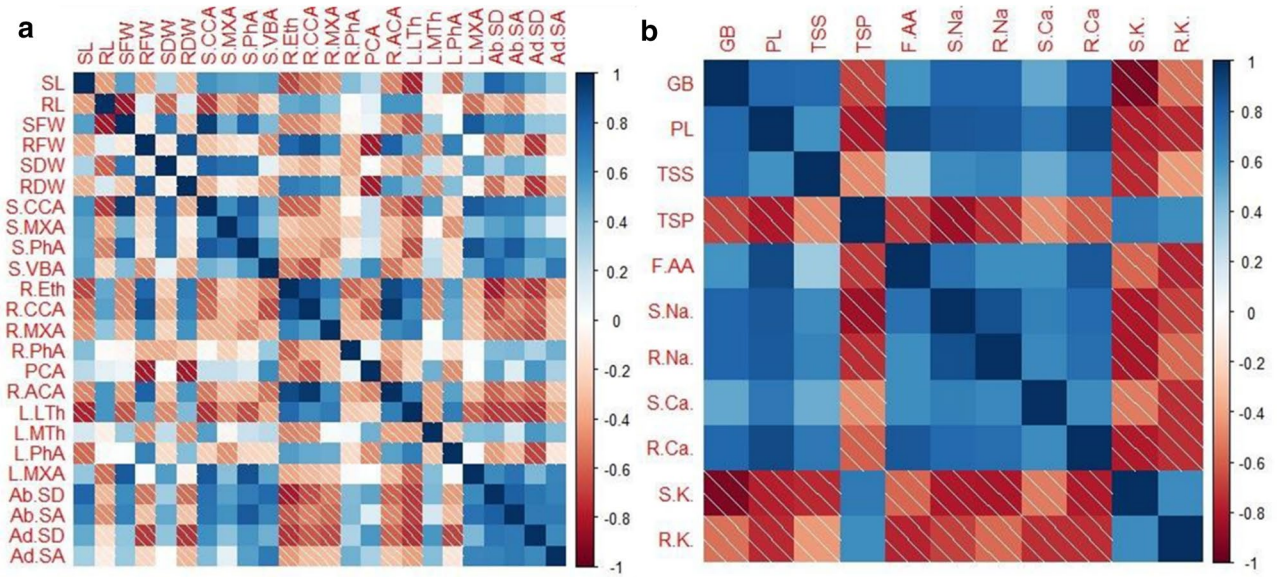

Fig. 9 **a** Correlation between morphological and anatomical traits **b** Correlation between ionic contents and organic osmolytes SL: shoot length , RL: Root length, SFW: shoot fresh weight, RFW: root fresh weight, SDW: Shoot dry weight, RDW: root dry weight, S.CCA: stem cortical cell area, S.MxA: stem metaxylem area, S.PhA : stem phloem area, S.VBA: stem vascular bundle area, R.Eth: root epidermis thickness, R.CCA: root cortical cell area, R.MxA: root metaxylem area, R.PhA: root phloem area, PCA: pith cell area, R.ACA: root aerenchyma area, L.LTh: leaf lamina thickness, L.MTh: leaf midrib thickness, L.PhA: leaf phloem area, L.MXA: leaf metaxylem area, AB.SD: Abaxial stomatal density, Ab.SA: abaxial stomatal area, Ad.SD: adaxial stomatal density, Ad.SA: adaxial stomatal area, GB: Glycine betaine, PL: Proline, TSS: Total soluble sugars, TSP: total soluble proteins, F.AA: Free amino acids, S.Na: shoot sodium, R.Na: root sodium, S.Ca: shoot calcium, R.Ca: root calcium, S.K: shoot potassium, R.K: root potassium

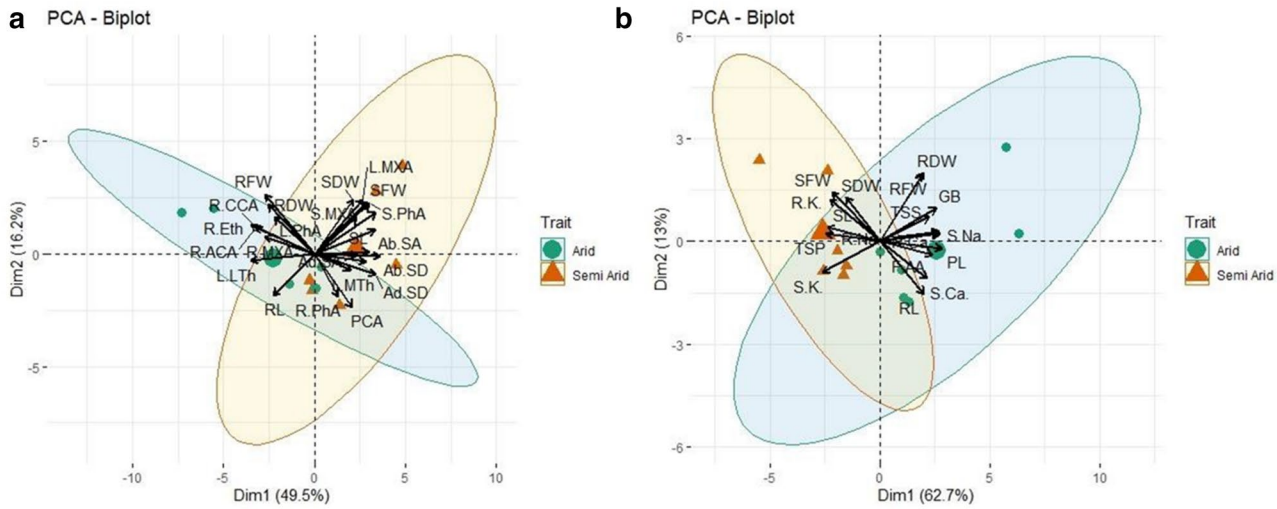

Fig. 10 **a** PCA bi-plot analysis between morphological and anatomical traits **b** Between morphological, physiological and ionic contents

more water. Similar findings were reported by Van den Berg and Zeng 2006 in *Heteropogon. contortus* grass that showed an increase in root biomass under extreme water deficit conditions. Plant ability to absorb water from deep soil is a very important factor in balancing water use and carbon assimilation during drought periods (Mansoor et al. 2019). Deep roots are required for small-statured crops like wheat, rice, and common bean (*Phaseolus vulgaris* L.) to extract nutrients from deeper soil water (Waseem et al. 2021). In this research, the root length was significantly increased in the QN population growing in extreme desert environments, which was also evident in *H. contortus*

(Van den Berg and Zeng 2006) under drought stress. The consistent increase in root length under arid conditions is an adaptive mechanism of many water deficit tolerant species which helps to go deeper into the soil to absorb more water (Abdel Razik et al. 2021). This justified the widespread distribution of species in aridity affected areas (Ahlem et al. 2023). Additionally, plant adaptation to water stress is a multifaceted phenomenon that affects plant growth development and overall productivity (Joshi et al. 2016). Markers associated with morphology, anatomy, physiology, and biochemistry are critical in investigating the changes to avoid severe water stress (Hameed et al. 2011).

Plant anatomical features are more prone to environmental stresses such as aridity and drought. (De Micco and Aronne 2012). Structural architecture and strategic behavior of plants play a crucial role in resisting water deficiency by modifying root, shoot, and leaf anatomical features (Sarwar et al. 2022).

Among root anatomical traits, a variable response was recorded in both arid and semi-arid regions. The arid zone populations exhibited an increase in root cortical cell area mainly due to storage parenchyma as aridity increased. Increased parenchymatous water storage tissues in the DF population from the arid zone provide additional space to retain moisture and cope with a longer period of dry conditions. Our findings support the hypothesis that larger cortical cells improve drought tolerance by lowering root metabolic costs, thereby allowing increased root growth and water absorption (Imran et al. 2021). Another modification is the presence of larger pith cells in the HR population of a semi-arid climate. Large, and loosely packed pith parenchymatous cells may retain water, which is crucial for survival during a prolonged period of water shortage (Zulfiqar et al. 2020).

The SA population from the arid zone had a significant increase in metaxylem vessels. Lage metaxylem vessels is another trait that is crucial for surviving in arid conditions. Larger vessels facilitate the movement of water, nutrients, and photosynthates through the root because of less resistance in the broader vessels (Mukhtar et al. 2013; Mumtaz et al. 2021a, b).

Aerenchyma tissues are of great ecological importance as they accelerate gaseous exchange, particularly in anoxia or hypoxia conditions (Akcin et al. 2017). Increased root aerenchyma cavities were observed in the DF population, collected from arid conditions. These cavities facilitate the water, nutrient, and salt translocation in different parts of plant (Singhal and Mehar 2020).

Vascular bundles play a vital role in water translocation which mainly depends upon the efficient flow of water inside metaxylem vessels (Horie et al. 2012). A significant decrease in stem vascular bundles and metaxylem vessels was recorded in most of the populations of arid zones particularly in DF and CA populations. This can be attributed to a high degree of drought tolerance and low resistance for water translocation (Horie et al. 2012; Purushothaman et al. 2013). The number and area of vascular bundles are normally correlated with biomass formation under harsh desert circumstances, because plants may devote more energy to survival than on normal vegetative development in harsh conditions (Bakhshandeh et al. 2020).

Leaf architectures exhibit great adaptability changing climatic conditions, often displaying climatic conditions, often displaying growth and structural features (Killi et al. 2017). Leaf anatomical adaptations like thick leaves, epidermal cells, and well developed bulliform cells had a strong relationship with tdrought tolerance (Kaleem and Hameed 2021; Mumtaz et al. 2021a, b). Herein bulliform cells were maximum in the DF population growing in areas with extreme high temperatures. Increasing bulliform cells help prevent water loss through the leaf surface in areas with extreme water shortages, as they cause the leaves to curl (Wasim et al. 2020). In all arid zone populations, the SA population displayed thickened midribs with a greater proportion of parenchymatous tissue, which assists in preventing water loss and protecting the plants from persistent dry weather (Anandan et al. 2018). A decline in stomatal density under harsh desert climates results in a reduced transpiration rate (Mansoor et al. 2019), thus a smaller number of stomata in arid zone populations like QN and DF might be extremely helpful in conserving water. Futhermore, smaller stomata size require less water to maintain turgor than larger ones (Mumtaz et al. 2019).

The adaptations of *C. ciliaris* to water stress were remarkable not only in terms of structural features but also in terms of functional behavior among different growing populations. In water stressed plants, plastid dysfunction disrupts the biosynthetic pathway for chlorophyll pigments, electron transport chain, and photosystem II reaction centers (Sun et al. 2020). Chl *a* is more sensitive to water deficit conditions, degrading more quickly as compared to Chl *b*. This can be explained by the fact that the reduction in Chlorophyll *a* seems to be the conversion to Chl *b* (Saeidi and Abdoli 2015). Water scarcity disrupts the photosynthetic apparatus including the destruction of mesophyll cell and epidermal tissues, leading to a decrease chlorophyll contents (Ahmad et al. 2007). As a result decrease in photosynthetic pigments (Chlorophyll and carotenoids) was more evident in arid populations of QN and DF.

Plants can change their water relation characteristics to regulate cellular functions in water-stressed conditions (Farooq et al. 2009; Al-maskri et al. 2014). As a result, plants adjust their osmotic balance by storing organic osmolytes like free amino acids, carbohydrates, sugars, and proline (Kaleem and Hameed 2021). Osmotic adjustments allow plants to maintain the turgor pressure and volume fraction

that is required to maintain metabolic processes (Shehzad et al. 2021). In our study, the accumulation of glycine betaine and proline was significantly higher in QN and DF populations growing in an arid climate. Plants accumulate glycinebetaine and proline as a defense mechanism to prevent turgor loss in conditions of low moisture, and this defense mechanism has previously been observed in species that are comparatively more tolerant, like *Vicia faba* L. (Gill et al. 2014). Proline concentration was enhanced in leaves of *Vigna radiata, Morus spp*., and *Arachis hypogea* under low water availability (Efeoğlu et al. 2009; Parida and Jha 2013; Gupta et al. 2014). Total soluble sugars were considerably increased in the semi-arid population, as reported by (Xia et al. 2021) in *Spartina alterniflora* under low availability of water, which may help them to survive in extended period of water scarcity.

Inorganic nutrients play a vital role in maintaining plants' growth and metabolism under stress conditions. Water scarcity typically reduces soil nutrient availability, root nutrient uptake, and translocation, and thus eventually reduces the ionic content in various plant tissues (Tadayyon et al. 2018). Primarily, it is due to reduced transpiration flow, which results in a decreased mass flow of soil water containing soluble nutrients i.e., potassium (K), nitrogen (N), and calcium (Ca) in roots (Zhai et al. 2015). Low water availability results in decreased potassium (K) absorption by plants (Hashmat et al. 2021). In the present study, potassium in the roots and shoots was significantly decreased in extremely arid environments. A similar finding was reported by (Wang et al. 2020) in *Malus hupehensis,* which showed a reduction in K uptake under drought stress. Changing stomatal movements and turgidity of guard cells due to water scarcity lead to lowered photosynthetic rate and reduced biomass as a result of lowered K content in leaves (Mumtaz et al. 2021a, b).

Conclusion

This study concludes that *C. ciliaris* has a number of variables that contribute significantly to the survival of this grass in the face of environmental adversities. Each population showed specific modifications based on anatomical and physiological features, demonstrating its adaptive strategy for ecological success in extreme aridity. The primary strategy for maintaining water conservation in more tolerant populations of QN and DF at the structural level was epidermal tissues, parenchyma tissues, and vascular tissues. At functional level plant ionic contents and osmolytes may allow this species to grow in extremely dry weather conditions. More importantly the formation of bulliform tissue was more obvious in arid zone populations DF, which help to prevent the excessive loss of wáter through transpiration during extreme arid conditions. One of the most frequent adaptive responses of plants to soil hypoxia and anoxia conditions was enhanced aerenchyma formation which regulate the exchnage of gases in response to abiotic stresses. Additionally, more tolerant QN and DF populations may serve as a foundation for restoring arid desert environments, not only in the desert itself but also in similar locations worldwide. Additonally, anatomical traits hold significant ecological importance and can be introduced into vulnerable species through genetic engineering techniques.

Supplementary Information The online version contains supplementary material available at https://doi.org/10.1007/s12298-023-01351-3.

Author contributions Conceptualization, AA, FA, and MH; Supervision, FA, MH, and KSA; Data curation, MKleem and SM; Formal analysis, NA, UI, AM, and MK; Investigation, AA and FA; Methodology, FA and MAS, and SM; Software, NA, UI, and FN; Writing—original draft, AA, and FA; Writing—review and Editing, KSA, AM.

Funding The authors did not receive support from any organization for the submitted work.

Availability of data and materials All data supporting the findings of this study are available within the paper and its Supplementary Information.

Declarations

Conflict of interest Authors declare that no conflict of interest exist with this manuscript. The authors have no relevant financial or non-financial interests to disclose.

References

Abdel Razik ES, Alharbi BM, Pirzadah TB, Alnusairi GS, Soliman MH, Hakeem KR (2021) γ-Aminobutyric acid (GABA) mitigates drought and heat stress in sunflower (*Helianthus annuus* L.) by regulating its physiological, biochemical and molecular pathways. Physiol Plant 172(2):505–527

Ahlem A, Lobna MF, Mohamed C (2023) Soil water leaf gas exchange and biomass production of Buffelgrass (*Cenchrus ciliaris* L.) with two ploidy levels under arid zone. Acta Ecol Sin 43(3):506–512

Ahmad ST, Haddad R (2011) Study of silicon effects on antioxidant enzyme activities and osmotic adjustment of wheat under drought stress. Czech J Genet Plant Breed 47(1):17–27

Ahmad MSA, Hussain M, Saddiq R, Alvi AK (2007) Mungbean: a nickel indicator, accumulator or excluder? Bull Environ Contam Toxicol 78(5):319–324

Ahmad KS, Wazarat A, Mehmood A, Ahmad MSA, Tahir MM, Nawaz F, Ahmed H, Zafar M, Ulfat A (2020) Adaptations in *Imperata cylindrica* (L.) Raeusch. and *Cenchrus ciliaris* L. for altitude tolerance. Biologia 75(2):183–198

Akcin TA, Akcin A, Yalcın E (2017) Anatomical changes induced by salinity stress in Salicornia freitagii (Amaranthaceae). Brazil J Bot 40:1013–1018

Al-Dakheel AJ, Hussain MI (2016) Genotypic variation for salinity tolerance in *Cenchrus ciliaris* L. Front in Plant Sci 7:1090

Ali T, Nafees M, Maqsood A, Naqvi SA, Shahzad U, Haider MS, Aslam MN, Shafqat W, Hameed M, Khan IA, Ahmar S (2020) Contribution of root anatomical characteristics in fruit profile of pomegranate genotypes to expand production area in Pakistan. Agron 10(6):810

Al-maskri A, Hameed M, Ashraf M, Khan MM, Fatima S, Nawaz T, Batool R (2014) Structural features of some wheat (*Triticum* spp.) landraces/cultivars under drought and salt stress. Arid Land Res Manag 28(3):355–370

Anandan S, Rudolph A, Speck T, Speck O (2018) Comparative morphological and anatomical study of self-repair in succulent cylindrical plant organs. Flora 241:1–7

Arnon DI (1949) Copper enzymes in isolated chloroplasts. Polyphenoloxidase in *Beta Vulgaris*. Plant Physiol 24(1):1

Asghar N, Akram NA, Ameer A, Shahid H, Kausar S, Asghar A, Idrees T, Mumtaz S, Asfahan HM, Sultan M, Jahangir I (2021) Foliar-applied hydrogen peroxide and proline modulates growth, yield and biochemical attributes of wheat (*Triticum aestivum* L.) Under varied n and p levels. Fresenius Environ Bull 30:5445–5465

Bakhshandeh E, Gholamhosseini M, Yaghoubian Y, Pirdashti H (2020) Plant growth promoting microorganisms can improve germination, seedling growth and potassium uptake of soybean under drought and salt stress. Plant Growth Regul 90(1):123–136

Baltas E (2007) Baltas Spatial distribution of climatic indices in northern Greece. A J Forecast Pract Appl Train Tech Model 14(1):69–78

Bates LS, Waldren RP, Teare ID (1973) Rapid determination of free proline for water-stress studies. Plant Soil 39(1):205–207

Berdugo M, Delgado-Baquerizo M, Soliveres S, Hernández-Clemente R, Zhao Y, Gaitán JJ, Gross N, Saiz H, Maire V, Lehmann A, Rillig MC (2020) Global ecosystem thresholds driven by aridity. Sci 367:787–790

Coscarelli RO, Gaudio RO, Caloiero T (2004) Climatic trends: an investigation for a Calabrian basin (southern Italy). IAHS 286:255–266

Efeoğlu B, Ekmekçi Y, Çiçek N (2009) Physiological responses of three maize cultivars to drought stress and recovery. S Afr J Bot 75(1):34–42

Farooq M, Wahid A, Kobayashi NSMA, Fujita, DBSMA, Basra, SMA (2009) Plant drought stress: effects, mechanisms and management. In: Sustainable agriculture. Springer, Dordrecht, pp 153–188

Fatima S, Hameed M, Ahmad F, Ashraf AR (2018) Structural and functional modifications in a typical arid zone species *Aristida adscensionis* L. along altitudinal gradient. Flora 249:172–182

Gill SS, Gill R, Anjum NA (2014) Target osmoprotectants for abiotic stress tolerance in crop plants—glycine betaine and proline. In: Plant adaptation to environmental change: Significance of amino acids and their derivatives, pp 97–108

Grieve CM, Grattan SR (1983) Rapid assay for determination of water soluble quaternary ammonium compounds. Plant Soil 70(2):303–307

Gupta SK, Bansal R, Gopalakrishna T (2014) Development and characterization of genic SSR markers for mungbean (*Vigna radiata* (L.) Wilczek). Euphytica 195:245–258

Hameed M, Ashraf M, Naz N (2011) Anatomical and physiological characteristics relating to ionic relations in some salt tolerant grasses from the Salt Range, Pakistan. Acta Physiol Plant 33:1399–1409

Hamid A, Singh S, Agrawal M, Agrawal SB (2020) Effects of plant age on performance of the tropical perennial fodder grass, *Cenchrus ciliaris* L. subjected to elevated ultraviolet-B radiation. Plant Biol 22:805–812

Hashmat S, Shahid M, Tanwir K, Abbas S, Ali Q, Niazi NK, Akram MS, Saleem MH, Javed MT (2021) Elucidating distinct oxidative stress management, nutrient acquisition and yield responses of *Pisum sativum* L. fertigated with diluted and treated wastewater. Agric Water Manag 247:106720

Horie T, Karahara I, Katsuhara M (2012) Salinity tolerance mechanisms in glycophytes: an overview with the central focus on rice plants. Rice 5(1):1–18

Hussain I, Saleem MH, Mumtaz S, Rasheed R, Ashraf MA, Maqsood F, Rehman M, Yasmin H, Ahmasghared S, Ishtiaq M, Anwar S (2022) Choline chloride mediates chromium tolerance in spinach (*Spinacia oleracea* L.) by restricting its uptake in relation to morpho-physio-biochemical attributes. J Plant Growth Regul 41:1594–1614

Imran M, Sun X, Hussain S, Rana MS, Saleem MH, Riaz M, Tang X, Khan I, Hu C (2021) Molybdenum supply increases root system growth of winter wheat by enhancing nitric oxide accumulation and expression of NRT genes. Plant Soil 459(1):235–248

Iqbal U, Hameed M, Ahmad F, Ahmad MSA, Ashraf M, Kaleem M, Shah SMR, Irshad M (2022) Contribution of structural and functional modifications to wide distribution of Bermuda grass *Cynodon dactylon* (L) Pers. Flora 286:151973

Javid K, Akram MAN, Ranjha MM, Pervaiz S (2020) GIS-based assessment of aridity over Punjab Province, Pakistan, by using climatic indices Arab. J Geosci 13(7):1–12

Joshi R et al (2016) Transcription factors and plants response to drought stress: current understanding and future directions. Front Plant Sci 7:1029

Kaleem M, Hameed M (2021) Functional traits for salinity tolerance in differently adapted populations of *Fimbristylis complanata* (Retz.). Int J Phytoremediation 23:1–14

Killi D, Bussotti F, Raschi A, Haworth M (2017) Adaptation to high temperature mitigates the impact of water deficit during combined heat and drought stress in C3 sunflower and C4 maize varieties with contrasting drought tolerance. Physiol Plant 159(2):130–147

Lian X, Piao S, Chen A, Huntingford C, Fu B, Li LZ, Huang J, Sheffield J, Berg AM, Keenan TF, McVicar TR (2021) Multifaceted characteristics of dryland aridity changes in a warming world. Nat Rev Earth Environ 2(4):232–250

Liu C, Li Y, Xu L, Chen Z, He N (2019) Variation in leaf morphological, stomatal, and anatomical traits and their relationships in temperate and subtropical forests. Sci Rep 9(1):1–8

Lowry OH (1951) Protein measurement with the Folin phenol reagent. J Biol Chem 193:265–275

Mansoor U, Fatima S, Hameed M, Naseer M, Ahmad MSA, Ashraf M, Waseem AFM (2019) Structural modifications for drought tolerance in stem and leaves of *Cenchrus ciliaris* L. ecotypes from the Cholistan Desert. Flora 261:151485

Marshall VM, Lewis MM, Ostendorf B (2012) Buffel grass (*Cenchrus ciliaris*) as an invader and threat to biodiversity in arid environments: a review. J Arid Environ 78:1–12

Mganga KZ, Kuhla J, Carminati A, Pausch J, Ahmed MA (2023) Leaf gas exchange characteristics, biomass partitioning, and water use efficiencies of two C4 African grasses under simulated drought. Grassland Rese 2(1):37–45

De Micco V, Aronne G (2012) Morpho-anatomical traits for plant adaptation to drought. In: Plant responses to drought stress. Springer, Berlin, pp 37–61

Moore S, Stein WH (1948) Photometric nin-hydrin method for use in the ehromatography of amino acids. J Biol Chem 176:367–388

Mukhtar N, Mansoor H, Muhammad A, Rashid A (2013) Modifications in stomatal structure and function in *Cenchrus ciliaris* L. and *Cynodon dactylon* (L.) Pers. in response to cadmium stress. Pak J Bot 45:351–357

Mumtaz S, Hameed M, Ahmad F, Sadia B (2019) Structural and functional modifications in osmoregulation for ecological success in purple nutsedge (*Cyperus rotundus*). Int J Agri Biol 22:1123–1132

Mumtaz S, Hameed M, Ahmad F, Ahmad MSA, Ahmad I, Ashraf M, Saleem MH (2021a) Structural and functional determinants of physiological pliability in kyllinga brevifolia rottb. for survival in hyper-saline saltmarshes. Water Air Soil Pollut 232:1–21

Mumtaz S, Saleem MH, Hameed M, Batool F, Parveen A, Amjad SF, Mahmood A, Arfan M, Ahmed S, Yasmin H, Alsahli AA (2021b) Anatomical adaptations and ionic homeostasis in aquatic halophyte *Cyperus laevigatus* L. under high salinities. Saudi J Biol Sci 28:2655–2666

Nawaz T, Hameed M, Ashraf M, Batool S, Naz N (2013) Modifications in root and stem anatomy for water conservation in some diverse blue panic (*Panicum antidotale* Retz.) ecotypes under drought stress. Arid Land Res Manag 27:286–297

Parida AK, Jha B (2013) Inductive responses of some organic metabolites for osmotic homeostasis in peanut (*Arachis hypogaea* L.) seedlings during salt stress. Acta Physiol Plant 35:2821–2832

Purushothaman R, Zaman-Allah M, Mallikarjuna N, Pannirselvam R, Krishnamurthy L, Gowda CLL (2013) Root anatomical traits and their possible contribution to drought tolerance in grain legumes. Plant Prod Sci 16(1):1–8

Rehman M, Liu L, Bashir S, Saleem MH, Chen C, Peng D, Siddique KH (2019) Influence of rice straw biochar on growth, antioxidant capacity and copper uptake in ramie (*Boehmeria nivea* L.) grown as forage in aged copper-contaminated soil. Plant Physiol Biochem 138:121–129

Ruzin SE (1999) Ruzin Plant microtechnique and microscopy. Oxford University Press, New York, p 322

Saeidi M, Abdoli M (2015) Effect of drought stress during grain filling on yield and its components, gas exchange variables, and some physiological traits of wheat cultivars. J Agric Sci Technol 17(4):885–898

Sarwar Y, Asghar A, Hameed M, Fatima S, Ahmad F, Ahmad MSA, Ashraf M, Shah SMR, Basharat S, Irshad IUM (2022) Structural responses of differentially adapted *Cenchrus setigerus* Vahl ecotypes to water deficit. Environ Exp Bot 194:104746

Shehzad M, Gul RS, Rauf S, Clarindo WR, Al-Khayri JM, Hussain MM, Munir H, Ghaffari M, Hussain NSM (2021) Development of a robust hydroponic method for screening of sunflower (*Helianthus annuus* L.) accessions for tolerance to heat and osmotic stress. Sci Rep 11:1–14

Singhal VP, Mehar SK (2020) Effect of limited nutrient availability on the development and relevance of root cortical aerenchyma. Plant Arch 20:1284–1288

Sun X, Chen F, Yuan L, Mi G (2020) The physiological mechanism underlying root elongation in response to nitrogen deficiency in crop plants. Planta 251(4):1–14

Tadayyon A, Nikneshan P, Pessarakli M (2018) Effects of drought stress on concentration of macro-and micro-nutrients in Castor (*Ricinus communis* L.) plant. J Plant Nutr 41:304–310

Van den Berg L, Zeng YJ (2006) Response of South African indigenous grass species to drought stress induced by polyethylene glycol (PEG) 6000. S Afr J Bot 72:284–286

Wang C, Zhao D, Qi G, Mao Z, Hu X, Du B, Liu K, Ding Y (2020) Effects of Bacillus velezensis FKM10 for promoting the growth of Malus hupehensis Rehd and inhibiting Fusarium verticillioides. Front Microbiol 10:2889

Waseem M, Mumtaz S, Hameed M, Fatima S, Ahmad MSA, Ahmad F, Ashraf M, Ahmad I (2021) Adaptive traits for drought tolerance in red-grained wheat (Triticum aestivum L.) landraces. Arid Land Res Manag 35:414–445

Wasim MA Naz N (2020) Anatomical adaptations of tolerance to salt stress in Cenchrus ciliaris L., a saline desert grass. J Anim Plant Sci 30

Wellburn AR (1994) The spectral determination of chlorophylls a and b, as well as total carotenoids, using various solvents with spectrophotometers of different resolution. J Plant Physiol 144(3):307–313

Wolf B (1982) A comprehensive system of leaf analyses and its use for diagnosing crop nutrient status. Commun Soil Sci Plant Anal 13:1035–1059

Xia H, Kong W, Liu L, Lin K, Li H (2021) Effects of harvest time and desalination of feedstock on *Spartina alterniflora* biochar and its efficiency for Cd^{2+} removal from aqueous solution. Ecotoxicol Environ Saf 207:111309

Yemm EW, Willis A (1954) The estimation of carbohydrates in plant extracts by anthrone. Biochem J 57:508

Zahid M, Rasul G (2012) Changing trends of thermal extremes in Pakistan. Clim Change 113(3):883–896

Zhai Q, Narbad A, Chen W (2015) Dietary strategies for the treatment of cadmium and lead toxicity. Nutrients 7:552–571

Zhang W, Wei J, Guo L, Fang H, Liu X, Liang K, Siddique KH (2023) Effects of two biochar types on mitigating drought and salt stress in tomato seedlings. Agronomy 13(4):1039

Zulfiqar F, Younis A, Riaz A, Mansoor F, Hameed M, Abideen ANAZ (2020) Morpho-anatomical adaptations of two *Tagetes erecta* L. cultivars with contrasting response to drought stress. Pak J Bot 52:801–810